CHARACTERIZATION OF ERYTHROMYCIN ESTERASES: A GENOMIC ENZYMOLOGY APPROACH TO MACROLIDE RESISTANCE

By

Kate L. Pengelly, B.Sc.

A Thesis

Submitted to the School of Graduate Studies

In Partial Fulfillment of the Requirements

for the Degree

Master of Science

McMaster University

MASTER OF SCIENCE (2010) McMaster University

(Biochemistry and Biomedical Sciences) Hamilton, Ontario

TITLE: Characterization of Erythromycin Esterases:
A Genomic Enzymology Approach to Macrolide Resistance

AUTHOR: Kate L. Pengelly, B.Sc. (University of Guelph)

SUPERVISOR: Professor G.D. Wright

NUMBER OF PAGES: viii, 86

Abstract

Enzymatic inactivation of antibiotics is a successful strategy employed by antibiotic resistant clinical pathogens. Genes coding for the antibiotic inactivating enzyme erythromycin esterase, or Ere, have been found in a variety of bacterial species, from clinical isolates to environmental soil-dwelling organisms. In order to better understand this family of proteins and this mode of macrolide resistance, four erythromycin esterases (EreA from *Providencia stuartii*, EreB from *E. coli,* and two putative Ere's from *Saccharopolyspora erythraea* and *Bacillus cereus*) were purified and characterized using a genomic enzymology approach. A robust quantitative enzyme assay was developed, and kinetic parameters for these different enzymes were compared. In the absence of a crystal structure for EreA or EreB, a model for EreB was developed based on the existing structure of the putative esterase from *B. cereus*. The importance of some conserved and potentially catalytic residues was examined using site-directed mutagenesis. Combined with mutagenesis, inhibitors, pH studies and solvent isotope effects were used to investigate potential enzyme mechanisms and two potential mechanisms were proposed for this family of proteins. A greater understanding of the function and mechanisms of antibiotic resistance elements such as the erythromycin esterases may provide valuable insights to aid in the ongoing struggle against resistant organisms in clinical settings.

Acknowledgements

First of all, I would like to thank my supervisor Gerry Wright for the opportunity to work on this project, and in such a great lab environment. Thank you Gerry for your guidance, encouragement, and ideas, and for always being excited to talk about science!

I would also like to thank the members of my committee for all their feedback and ideas for this project. Thank you to Alba Guarné for her guidance and for assistance with crystallization trials, and thank you to Brian Golding for creating alignments and for keeping the Wright lab's phylogeny on the right track. Your expertise in crystallography and bioinformatics was incredibly helpful.

To the Wright lab members, past and present, thank you for your support and friendship, for the opportunity to learn from you and with you, and for all the lunch discussions and cooking competitions. A special thank you to Kalinka Koteva for her help with the mass spectrometry and all things chemistry, and for her support and encouragement throughout my time in the lab. Another special thank you to Maria Morar, for the modelling of EreB, and for all her help and support with this project.

Finally, thank you to Chris and to my family for your love and support, always.

List of Figures:

List of Tables:

Chapter 1 – Introduction

1.1 Introduction

In the last sixty years, the use of antibiotics has dramatically reduced the number of deaths that occur annually due to infectious disease (31). However, the rise of organisms resistant to commonly used antibiotics continues to be a significant and growing medical problem (27). Resistant bacteria use a number of strategies to overcome the effect of antibiotics, including efflux, target modification, and drug modification (50). This latter mechanism of resistance involves the production of an enzyme that modifies the antibiotic so it is no longer active against its cellular target. One such enzyme capable of degrading the antibiotic erythromycin and abolishing its antibacterial activity is erythromycin esterase, or Ere. The objective of this project is to express, purify, and characterize a number of erythromycin esterases from a variety of source organisms. We hope to elucidate some structural and mechanistic features of these enzymes. The more that is known about the enzymes involved in antibiotic resistance, the more information we have to aid us in the ongoing struggle against resistant pathogenic organisms.

1.2 Erythromycin and its semi-synthetic derivatives

Erythromycin is produced by the soil dwelling organism *Saccharopolyspora erythraea,* isolated in the Philippines, and was introduced clinically in 1952 (48). Erythromycin belongs to the wider family of macrolide drugs, which share a characteristic lactone ring, but differ in the size of the ring, and the substitutions at various positions (see Figure 1-1). Since the introduction of erythromycin, chemical modifications to the naturally produced macrolides have yielded semi-synthetic drugs with improved pharmacokinetic properties, improved efficacy, and reduced ability to

induce resistance mechanisms. For example, clarithromycin has a methoxy group at C6, giving it improved acid stability, while azithromycin has an expanded ring structure and possesses both improved acid stability and increased activity against some Gram-negative species (32, 44). The ketolide telithromycin shares the methoxy group at C6 with clarithromycin, but has a ketone group at C3 in place of the cladinose sugar, and a large aromatic carbamate extension at C11/C12. As a result of these additional modifications, telithromycin has improved binding to its ribosomal target, and does not induce expression of the *erm* genes commonly involved in resistance(3).

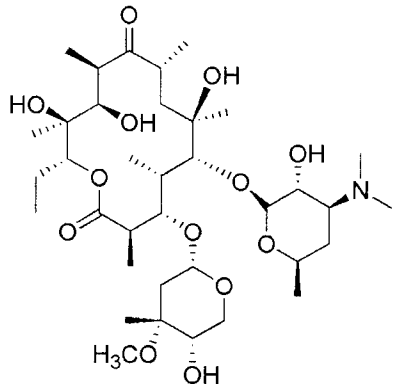

Erythromycin A

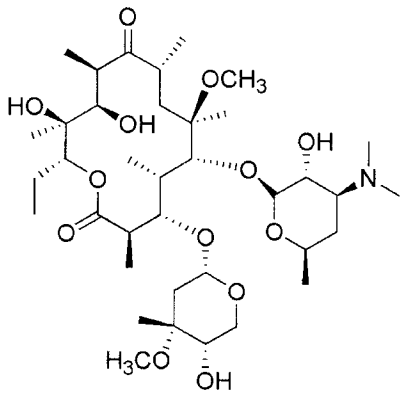

Clarithromycin

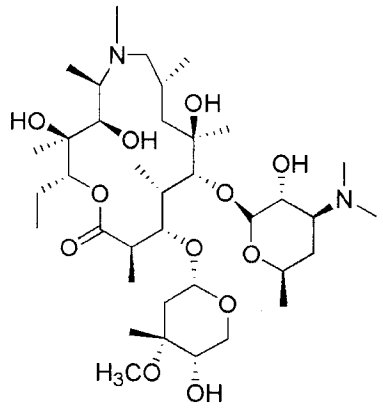

Azithromycin

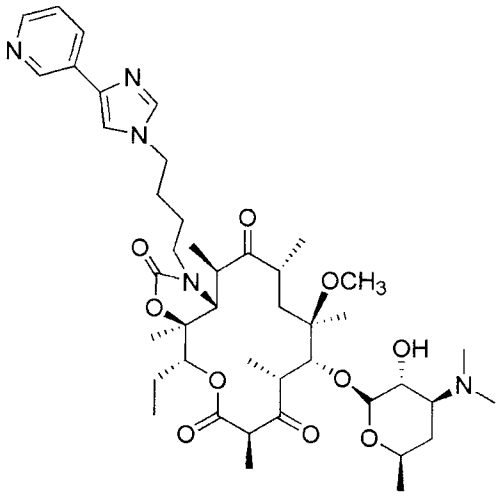

Telithromycin

Figure 1-1. Chemical structures of some macrolide antibiotics, including the natural compound erythromycin, the 15-membered azithromycin, and other semi-synthetic derivatives clarithromycin and ketolide telithromycin.

The cellular target of macrolides, as with a host of other antibiotics, is the prokaryotic ribosome. Erythromycin works by binding reversibly to the 50S subunit and inhibiting protein synthesis. It blocks the peptide exit tunnel, and is able to stop the growing polypeptide chain from leaving the ribosome, causing a static effect on bacterial growth (16, 41). In addition, erythromycin has been shown to increase the rates of dissociation of peptidyl tRNA from the ribosome (28), and to have an inhibitory effect on assembly of the 50S ribosome (12).

Erythromycin and its derivatives are active against Gram-positive staphylococci, streptococci, bacilli, as well as against some Gram-negative human pathogens including *Haemophilus influenzae*, *Bordatella spp.*, *Legionella spp.*, and *Chlamydia spp.* (10). Erythromycin is especially used to treat respiratory tract infections and community acquired pneumonias, and is still widely prescribed today due to its safety and efficacy (42).

1.3 Macrolide Resistance

1.3.1. Modes of Resistance

In 1952, the first year that erythromycin was introduced, the first cases of clinical resistance were recorded (32). Macrolide resistance continues to be a growing problem today. A recent study revealed that 30% of *Streptococcus pneumoniae* clinical isolates in 2004 were macrolide resistant, up from 10% in 1994, and only 0.2% in the late 1980's (15). Resistance mechanisms to macrolides are varied (see Table 1-1). For example, if a key adenine (A2058) of the 23S rRNA is substituted for a cytosine, then erythromycin can no longer bind its target, and protein synthesis can proceed unhindered. Similarly, if A2058 is methylated by a ribosomal methyltransferase enzyme encoded by the *erm*

genes, erythromycin binding is blocked, and resistance is conferred. Erythromycin itself can be modified by the addition of a phosphate group added by a macrolide phosphotransferase enzyme, or the drug can be hydrolyzed by an erythromycin esterase enzyme encoded by *ere*. It is this latter mechanism of drug hydrolysis that is of particular interest here.

Table 1-1. Some examples of resistance mechanisms employed by bacteria to confer macrolide resistance and the genes or mutations responsible

Type of resistance mechanism	**Mode of action**	**Examples of genes or mutations responsible**	**Reference**
target modification	- methylation of ribosome at key adenine positions on 23S rRNA	*erm*	(54)
target mutations	- mutations of ribosomal rRNA	A2058C or A2058U	(21)
	- ribosomal protein L22 and L4 mutations	G66C, ΔMKR	(53)
efflux	-efflux of drug through use of an ATP dependent pump	*msr, erp, mef, mre*	(37)
drug modification	-phosphorylation of drug	*mph*	(35)
	-glycosylation of drug	*mgt, oleI, oleD*	(11, 13)
drug degradation	-hydrolyisis of lactone ring	*ere*	(8)

1. 3.2 Erythromycin esterases

In the early 1980's Courvalin and his group at the Pasteur Institute were working with a clinical isolate of *Escherichia coli* that was highly resistant to erythromycin (minimum inhibitory concentration or MIC >2mg/mL). It was found that this strain could inactivate erythromycin, and it was proposed that the inactivation occurred via hydrolysis of the lactone ring. The gene responsible for conferring resistance

was found to be plasmid borne with a GC content similar to that of *E. coli*, and was named *ere* for erythromycin esterase (8).Courvalin *et al.* then examined other clinical enterobacteria strains that could inactivate erythromycin. They found an *E. coli* strain that produced the same inactivation product, but when colony hybridization with an *ere* probe was carried out, no hybridization was seen. The new gene responsible for the resistance phenotype was also found to be plasmid borne, and similar in size (about 1.3 kb) compared with the first *ere* gene (now designated *ereA*). However, it was found that the two genes were only 17% identical when the DNA sequences were compared (6). From examining the GC content and codon usage in this new *ereB* gene, it was proposed that *ereB* was of exogenous origin to *E. coli* and had likely been acquired from a Gram-positive organism (4, 5). In the current literature, a gene similar in sequence to the *E. coli* *ereA* gene by >80% is designated *ereA* (43), while any other gene with predicted erythromycin esterase activity may be annotated as an *ereB*, or an erythromycin esterase type II.

Since these early investigations, other clinical isolates have been found to possess erythromycin inactivating activity. For example, a strain of *S. aureus* was found to inactivate erythromycin as well as other 14- and 16-membered macrolides (49). Isolates of *E. coli* in Japan were found to inactivate erythromycin as well as the newer semi-synthetic drugs clarithromycin and azithromycin through hydroylsis of the lactone ring (33, 36). An isolate of *Providencia stuartii* was found to contain an *ereA* gene within a class I integron (40), while other *E. coli* isolates contain *ereA* within a class II integron (9). Recently, sequencing of a multidrug resistant clinical isolate of *Klebsiella pneumoniae* from India revealed an *ere* gene sharing 92% nucleotide sequence identity

with *ereA*, and was designated as *ereC* (52). As with *ereA* genes previously studied, this gene was also located within a class I integron, along with various other antibiotic resistance genes, *arr-2* (rifampin resistance), *aadA1* (gentamicin resistance), *cmlA7* (chloramphenicol). Although the prevalence of macrolide hydrolysis as a mechanism of resistance is still relatively rare (*erm* mediated ribosomal methylation is the mechanism most often responsible for erythromycin resistance in clinical settings), the fact that the *ere* genes are so often found within mobile genetic elements means there is the possibility of this mechanism becoming more prevalent in the future.

In addition to clinical isolates from hospital patients, *ere* genes are found in a variety of other bacterial species. The genome of the producing organism for erythromycin, *Saccharopolyspora erythraea*, was sequenced in 2007 and was found to contain two copies of an *ere* gene (38). One copy was located within the erythromycin biosynthetic gene cluster (SACE_0712), but is likely inactivated by the insertion of a transposable element, and in transcriptional studies was not found to be expressed in the presence of erythromycin (39). Another predicted erythromycin esterase (SACE_1765) remains intact and is located outside of the cluster, elsewhere in the genome. Other environmental organisms such as *Streptomyces coelicolor, Rhodococcus sp. RHA1, Bacillus cereus,* and *Mesorhizobium sp. BNC1* contain putative erythromycin esterase homologues. It is yet unclear how many of the putative erythromycin esterases are truly acting as resistance determinants in cells. It may be that these hypothetical proteins do have the potential to confer resistance if expressed, or they may have some other cellular function.

A *Pseudomonas* species isolated from a Washington fish hatchery produced an erythromycin inactivating enzyme whose N-terminal sequence was very similar to the expected *E. coli ereA* gene product (25). The 51 kDa protein having this activity was purified and some initial characterization was performed, including steady state kinetics, analysis of substrate specificity, pH dependence, temperature stability, as well as some preliminary investigations into possible enzyme inhibitors. Prior to the work described in this thesis, no *ereB* encoded enzyme had been purified or characterized, and although the products of the reactions catalyzed by EreA and EreB enzymes are indistinguishable, it is unknown whether the enzymes carry out the same reactions via the same mechanism.

Understanding interactions between an antibiotic and its biological target, and just how resistance mechanisms work to overcome this interaction, may yield the opportunity to design better drugs for clinical therapy. The discovery of inhibitors for enzymatic mechanisms of resistance may lead to the development of compounds that can be co-administered with the antibiotic in a combination therapy, at once attacking the pathogenic organism and its ability to defend itself.

1.4 Rationale Behind Selection of Genes

In choosing which erythromycin esterases to work with, a variety of factors were considered. A combination of genes annotated as *ereA* and *ereB* was desirable, in order that any differences between these two types might be determined. Previously, our lab had obtained a plasmid containing an *ereA* from a multidrug resistant clinical isolate of the enterobacteria *Providencia stuartii*. Since the sequence of this *ereA* is very similar to that of the *E. coli ereA* originally studied by Courvalin (8), and was similar in amino acid sequence to the protein studied by Kim *et al.* (25), this *ereA* was selected for initial study.

In addition, an *E. coli* strain harbouring a plasmid containing the *E. coli ereB* was obtained from Patrice Courvalin. Along with these esterases having known activity, three putative *ere* genes were selected, one from the resistant producing organism, *Saccharopolyspora erythraea* (SACE_1765) and one from the erythromycin sensitive organism *Streptomyces coelicolor* (SCO_3588). The third putative *ere* selected was from a sequenced strain of *Bacillus cereus* ATCC 14579 (23). This gene, BC_3205, corresponds to the gene product Bcr136, identified as a target by the Northeast Structural Genomics Consortium (NESG) and has been successfully purified, crystallized, and its 3D structure determined (PDB 2QGM). Although this gene was machine annotated as a "succinoglycan biosynthesis" protein, it shares sequence identity of 88-98% to other genes in *B. thuringenisis* and other *B. cereus* species that have been annotated as putative erythromycin esterases. Although its sequence identity at the amino acid level, when compared to *E. coli* EreB is only about 25% (43% similarity), this is comparable to the amount of conservation seen between other Ere's. The fact that a 3D structure exists for this protein, and the conservation of key residues that are shared between other putative and known esterases, made this a protein of interest.

In terms of genetic context, the *ereA* and *ereB* selected were located within mobile genetic elements, and originally discovered in clinical gram-negative isolates. In contrast, the other genes selected were all found within the genomes of environmental gram-positive species. Since the genomes of these organisms have been sequenced, it is possible to examine the genetic context within which these potential resistance elements were found. The selected gene from *S. erythraea*, hereafter known as *ere*-se, was not located within the biosynthetic cluster for erythromycin. An examination of genetic

context did not reveal the presence of any other predicted resistance proteins, although several genes encoding for transposases were present in the surrounding region. For *S. coelicolor*, the surrounding region did encode for some other genes relating to antibiotic resistance, namely vancomycin resistance determinants *vanH, vanA* and *vanX*, and the two-component regulatory system (*vanR, vanS*) that regulates expression of these genes (24). This was interesting as the strain used for cloning the *ere*-sc gene (*S. coelicolor* M 145) was found to be resistant to vancomycin, although sensitive to erythromycin. The surrounding region of the *B. cereus* putative *ere* (*ere*-bc) revealed the presence of one other resistance determinant, *tetV*, encoding for a tetracyline efflux pump.

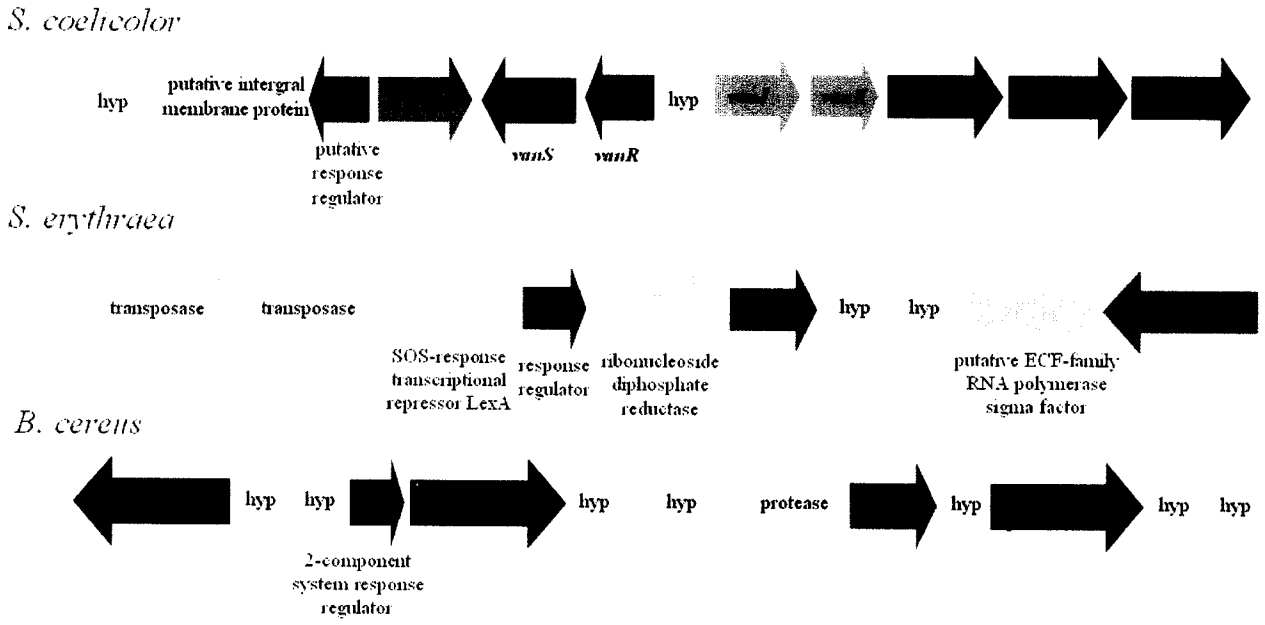

Figure 1-2. Genetic context of *S. coelicolor, S. erythraea*, and *B. cereus* putative erythromycin esterases, adapted from (1)(2), and (38).

1.5 Project Aim and Approach

The aim of this project has been to clone, express, purify, and characterize both verified and putative erythromycin esterases from a variety of source organisms. A genomic enzymology approach will be applied to the problem of better understanding erythromycin resistance. This approach combines enzyme kinetics, structural information obtained from crystallographic studies, and the use of bioinformatics tools to find potentially homologous proteins for further comparison. The ability to inactivate erythromycin through hydrolysis was confirmed for the known erythromycin esterases EreA and EreB, and was investigated for the predicted esterases. A robust quantitative enzyme assay was developed, and kinetic parameters for these different enzymes was compared. In the absence of a crystal structure for EreA or EreB, a model for EreB was developed based on the existing structure of the putative esterase from *B. cereus*. The importance of some conserved and potentially catalytic residues was examined using site-directed mutagenesis. Combined with mutagenesis, inhibitors, pH studies and solvent isotope effects were used to investigate potential enzyme mechanisms for both EreA and EreB. Greater understanding of the function and mechanisms of antibiotic resistance elements may provide valuable insights to aid in the ongoing struggle against resistant organisms in clinical settings.

Chapter 2 – Purification and comparison of function for selected erythromycin esterases

2.1 Overview

The selected erythromycin esterases, both known and putative, were cloned into suitable expression vectors, and the expression and solubility of these proteins was examined. With the exception of the putative esterase from *Streptomyces coelicolor*, these proteins were successfully purified, either with metal affinity chromatography (*S. erythraea* and *B. cereus* Ere proteins), or with a combination of anion exchange and hydrophobic interaction chromatography (EreA from *P. stuartii* and EreB from *E. coli*). For the esterase from *S. coelicolor,* soluble protein was not able to be obtained.

The ability of each of these esterases to function as true antibiotic resistance elements, both in cells and in vitro as purified proteins, was examined. Their activity against various macrolide drugs used clinically was also investigated. It was next necessary to develop a quantitative assay in order to better compare the activity of these different proteins, and to this end, a number of different strategies were employed, including synthesis of chromogenic esterase substrates, the use of thin-layer chromatography and radiolabelled [^{14}C] erythromycin, and detection of reactants and products via liquid chromatography/mass spectrometry. A continuous spectrophotometric assay using the commercially available chromogenic esterase substrate *p*-nitrophenyl butyrate was developed and used to obtain kinetic parameters for the enzymes.

2.2 Materials and Methods

2.2.1 General Methods

Analysis of DNA was done using 1% Tris-acetate-ethylenediamine-tetracetic acid (TAE agarose gels, stained with 1:500 Sybr Safe DNA stain solution (Invitrogen, Burlington). Gels were scanned with the Typhoon™ variable mode imager. DNA sequencing and oligonucleotide primer synthesis was performed by the Mobix Facility (McMaster University). Plasmids were propagated in *E. coli* Top10 cells, while *E. coli* BL21 (DE3) cells were used for protein overexpression. Cell cultures were grown in Luria-Bertani (LB) broth supplemented with either 100 μg/ml ampicillin or 50 μg/ml kanamycin, depending on the plasmid selection marker. Protein purification was performed using the AKTA Explorer system (GE Healthcare), with all columns and resin purchased from GE Healthcare unless otherwise stated.

Erythromycin, clarithromycin, azithromycin, and roxithromycin were purchased from Sigma-Aldrich, and working stocks of 2.5 mg/mL were made up in either 100% ethanol (erythromycin, roxithromycin) or DMSO (clarithromycin, azithromycin). Telithromycin was obtained from Aventis Pharmaceuticals Inc. in solid tablet form. Pills containing 5 mg telithromycin each were crushed using a mortar and pestle, resuspended in 5 mL of 100 % ethanol, and insoluble particulates were removed by centrifugation to make a 1 mg/mL stock solution, which was then stored at 4°C.

2.2.2 Gene Amplification and Plasmid Construction

Plasmid DNA containing *ereA* isolated from *Providencia stuartii*, and *ereB* from *E. coli* were generously donated by Paul Roy (Université Laval, Ste-Foy, Québec, Canada) and Patrice Courvalin (Institut Pasteur, Paris, France) respectively. Genomic

DNA from *S. erythraea* and *S. coelicolor* was isolated in-house by Vanessa D'Costa. Primers for *ere* gene amplification were designed to include attB1 and attB2 sites (see Table 2-1) in order to facilitate recombination into downstream Gateway® vectors (Invitrogen, Carlsbad, CA). Restriction sites were also included to facilitate later ligation into pET vectors (Novagen). Genes were amplified using PCR, and resulting 1.2 kb fragments were subsequently incorporated into pDONR201, then pDEST14 (*ereA, ereB, and ere-se*) or pDEST17 (*ere-se, ere-sc*) Gateway® vectors. pDEST14 allowed for expression of native, untagged protein, while pDEST17 allowed for the expression of N-terminal hexa-His fusion proteins. An expression construct for Bcr136, a putative esterase from *B. cereus* was generously donated by Gaetano Montelione (Rutgers University, New Jersey, Northeast Structural Genomics Consortium). This construct allowed for the overexpression of C-terminally hexa-His tagged protein.

Table 2-1. Primers used for the amplification of *ere* genes

Gene	Primer pair(5'→3')
ereA	Forward 5'-GGGACAAGTTTGTACAAAAAAGCAGGCTTC**GAAGGAGATA**GA [redacted]**ACATGGAGAACGACCAGAAC** – 3' Reverse 5'-GGGGACCACTTTGTACAAGAAAGCTGGGTC[redacted]**TAGGGC** **AACCAGGCTGTCC** – 3' Reverse, no STOP 5' – GGGGCCACTTTGTACAAGAAAGCTGGGT[redacted]**GTAGGGCAACC** **AGGCTGTCCTTGCC** – 3'
ereB	Forward 5' –GGGGACAAGTTTGTACAAAAAAGCAGGCTTC**GAAGGAGATA**GA [redacted]**AGGTTCGAAGAATGGGTC** – 3' Reverse 5' – GGGGACCACTTTGTACAAGAAAGCTGGGTC[redacted]**TAGGGC** **AACCAGGCTGTCC** – 3' Reverse, no STOP 5' – GGGGACCACTTTGTACAAGAAAGCTGGGT[redacted]**GTTCATAAA** **CGACCTCAGATACAG** – 3'
ere-sc	Forward 5' - GGGGACAAGTTTGTACAAAAAAGCAGGCTTC[redacted]**TCCCGCAC** **GGTGATCCGC** – 3' Reverse 5' – GGGGACCACTTTGTACAAGAAAGCTGGGTC[redacted]**GCGGTA** **GCTCTGACCGTCCTTG** – 3'
ere-se	Forward 5' - GGGGACAAGTTTGTACAAAAAAGCAGGCTTC[redacted]**GCGGCA** **GCGTCGATCCGTG** – 3' Reverse 5' – GGGGACCACTTTGTACAAGAAAGCTGGGTC[redacted]**GCGTTC** **GGTGGGGTTGGCCGG** – 3'

Legend:

Gateway attB1/attB2 sites [redacted]

Shine-Dalgarno sequence [redacted]

[redacted] [redacted]

Gene specific region

2.2.3. Protein Solubility Assays

Expression constructs were transformed into *E. coli* BL21 cells and expression and solubility of each protein was assessed by sodium dodecyl sulfate polyacrylamide gel electrophoresis (SDS-PAGE) prior to large-scale purification. A 25 mL culture was inoculated 1/100 from an overnight culture of *E. coli* BL21 cells harbouring different expression plasmids, and incubated at 37°C with shaking at 250 rpm. After an optical density (OD_{600}) of 0.6 was reached, 1 mL of culture was removed and frozen, while the remaining culture was divided into three aliquots of 6 mL after the addition of isopropyl β-D- thiogalactopyranoside (IPTG) to 1 mM. One culture was grown at 16°C overnight, one at 24°C for 5 hours, and one at 37°C for three hours. After the appropriate times had elapsed, cells were collected by centrifugation, and were resuspended in lysis buffer (20 mM Tris pH 8.0, 1.4 mM 2-mercaptoethanol, and 0.05 % lauryldimethylamine-oxide). Cells were lysed with the addition of lysozyme to 1 mg/mL, and incubation on ice for 30 minutes. Centrifugation was used to separate cell debris from soluble protein in the cell lysate, and pellets and supernatants were then analyzed by SDS-PAGE.

2.2.4. Expression and Purification

Expression plasmids were transformed into *E. coli* BL21 (DE3) Rosetta (Novagen, Darmstadt, Germany) cells for overexpression under the T7 promotor. Cells were grown in 1L Luria-Bertani broth at 37°C until an optical density of 0.6 at 600 nm was reached. Protein expression was induced by the addition of IPTG to a final concentration of 1 mM, and cells were then grown overnight at 16°C. Harvested cells were washed in a 0.1% NaCl solution, resuspended in 25 mL of lysis buffer (50 mM

HEPES pH 7.5, 1 mM EDTA, 1 mM phenylmethanesulfonyl fluoride; 1 mM DNaseI), and lysed at 30 kPSI using a cell disrupter (Constant Systems, UK).

2.2.4.1. Purification of EreA, EreB, and putative esterase from *S. erythraea*

After centrifugation of cell lysate, supernatant was applied directly to an XK 26/20 HiPrep Q Sepharose column at a flow rate of 1 ml/min. Protein eluted at 30% buffer B (50 mM HEPES pH 7.5, 1mM EDTA, 1 M NaCl, 5% glycerol). Fractions containing erythromycin esterase activity were pooled and 3 M ammonium sulfate solution was added to a final concentration of 1 M. Precipitant was removed by centrifugation at 20 000 rpm, and resulting supernatant was applied to an XK 16/20 HiPrep Phenyl-Sepharose column equilibrated with buffer A (50 mM HEPES pH 7.5, 1 mM EDTA, 1 M ammonium sulfate, 5 % glycerol) . Protein eluted from this column at 100 % buffer B (50 mM HEPES pH 7.5, 1 mM EDTA, 5% glycerol). Fractions containing esterase activity were pooled and concentrated to approximately 10 mg/ml before being applied to a Superdex 200 column equilibrated with 50 mM HEPES pH 7.5, 0.1 mM EDTA, 150 mM NaCl, and 5% glycerol. Fractions containing Ere were then pooled, concentrated to 2 mg/ml and stored at either 4°C and used within 3 days, or frozen with 20% glycerol at -20°C and stored for up to 6 months without loss of activity.

2.2.4.2. Purification of putative erythromycin esterases from *B. cereus*

The supernatant after cell lysis and centrifugation was applied to a 5 mL Ni-NTA column (QIAGEN, Valencia, CA) at a flow rate of 1 ml/min. Protein was eluted at 30% buffer B (50 mM HEPES pH 7.5, 250 mM imidazole, 30 mM NaCl). Fractions containing protein having the correct size as determined by SDS-PAGE were pooled and dialyzed against 50 mM HEPES pH 7.5, then brought to approximately 10 mg/mL.

Protein was further purified by gel filtration using a Superdex 200 gel filtration column. Purified protein was concentrated to 2 mg/ml and stored at either 4°C and used within 3 days, or frozen with 20% glycerol at -20°C and stored for up to 6 months, as with EreA and EreB.

Table 2-2 Summary of columns and buffer conditions used for the purification of Ere enzymes

Protein	**EreA, EreB, Ere-se**	**Ere-bc**
Column 1	HiPrep Q Sepharose XK 26/20	Ni-NTA 5 mL Superflow Cartridge
Buffer A	50 mM HEPES pH 7.5 1 mM EDTA 5% glycerol	50 mM HEPES pH 7.5 10 mM imidazole 30 mM NaCl
Buffer B	50 mM HEPES pH 7.5 1 M NaCl 1 mM EDTA 5% glycerol	50 mM HEPES pH 7.5 250 mM imidazole 30 mM NaCl
Column 2	HiPrep Phenyl-Sepharose XK 16/20	HiLoad 26/60 Superdex-200
Buffer A	50 mM HEPES pH 7.5 1 M Ammonium sulfate 1 mM EDTA 5% glycerol	50 mM HEPES pH 7.5 0.1 mM EDTA 150 mM NaCl 5% glycerol
Buffer B	50 mM HEPES pH 7.5 1 mM EDTA 5% glycerol	-
Column 3	HiLoad 26/60 Superdex-200	-
Buffer A	50 mM HEPES pH 7.5 0.1 mM EDTA 150 mM NaCl 5% glycerol	-

Removal of the N-terminal His tag from Ere-bc was achieved through thrombin cleavage. Pooled fractions containing Ere-bc were dialyzed against thrombin cleavage buffer (20 mM Tris pH 8.0, 150 mM NaCl, 2.5 mM $CaCl_2$ and 0.1% 2-mercaptoethanol) and an overnight incubation of 1:500 thrombin to protein ratio was performed at room temperature. Uncleaved protein was removed by passing the reaction through a 5 mL Ni-

NTA column and collecting the unbound material. Gel filtration was then used to further purify the untagged protein.

2.2.5. Ability of cells expressing known and putative erythromycin esterase genes to grow in the presence of erythromycin

Minimum inhibitory concentrations (MIC) for erythromycin against cells expressing the various erythromycin esterase enzymes were determined by broth dilution method in LB broth media. Colonies of *E. coli* BL21 (DE3) cells harbouring expression plasmids for each protein were resuspended in 0.85 % sterile saline solution to an OD_{625} of 0.8-0.1. This solution was diluted 1/10 in sterile LB broth twice, to a final dilution of 1/100. 50 μL of this cell suspension was added to sterile 96-well plates containing 50 μL dilutions of erythromycin in LB broth ranging from 8-2048 μg/ml. Plates were incubated at 37°C overnight and the MIC was defined as the lowest concentration of drug having no growth present after 16 hours.

2.2.6. Activity of purified proteins against a panel of macrolide antibiotics using an inactivation bioassay

The ability of purified esterases to inactivate erythromycin was tested using a Kirby-Bauer disc diffusion assay as previously shown (14). To assess antibiotic inactivation, purified enzyme was incubated with 25 μg/mL macrolide for 1 hour at 24°C, the reaction stopped with addition of methanol to 50 % (v/v), and precipitated protein was removed by centrifugation. A petri dish was inoculated with a lawn of the macrolide susceptible organism *Micrococcus luteus*, and 10 μL of supernatant from the reaction was spotted onto a sterile paper disc placed on the agar. After two days of growth, no zone of inhibition was seen around the disc with enzymatically inactivated erythromycin, compared to that spotted with erythromycin alone.

2.2.7. Analysis of inactivation products by liquid chromatography/mass spectrometry

Liquid chromatography/mass spectrometry (LC/MS) was used to detect the inactivation products of erythromycin by EreA and EreB, and confirm that the product was, in fact, hydrolyzed erythromycin. This was performed using an Applied Biosystems QTRAP LC/MS/MS (Boston, MA), and the following conditions. 50 uL reactions of 0.08 mg Ere with 25 μg/mL macrolide were allowed to proceed at room temperature for up to 24 hours. Reactions were stopped with the addition of 3 volumes cold acetonitrile and placed on ice for 5 minutes. Centrifugation was performed to remove any precipitated protein, and 100 μL samples were prepared by addition of 50 μL acetonitrile to a 50 μL aliquot from the stopped reaction. Separation was achieved with reverse phase liquid chromatography using a C18 column (Dionex, Acclaim™120, 3 μm, 120 Å, 4.6 x 150 mm), and the following method : 0-5 minutes 5% solvent B; 5-25 minutes linear gradient up to 97% solvent B; 25-28 minutes 5% solvent B; 0.05% formic acid (v/v) (Solvent A), acetonitrile/0.05% formic acid (v/v) (Solvent B) and a flow rate of 1 ml/min.

2.2.8. Assay development

Although the disc diffusion assay described above was sufficient for determining if Ere proteins were active, a robust and quantitative assay was required for kinetic and substrate specificity information to be obtained, and to allow for the comparison of activity between different enzymes. Erythromycin as a substrate poses a problem for assay design, as it is not coloured, and has no characteristic absorbance wavelength, making it difficult to detect in a continuous assay using a cuvette or 96-well plate format. To overcome these problems, a number of different approaches were taken, including the use of liquid chromatography/mass spectrometry (LC/MS), radiolabelled [^{14}C]-

erythromycin and thin-layer chromatography, as well as a continuous assay with the chromogenic substrate *p*-nitrophenyl butyrate.

2.2.8.1 Optimization of LC/MS for use in a quantitative assay

Some optimization of this method for use as a quantitative assay was performed. At first glance, an approach relying on mass would seem to be ineffective with erythromycin as a substrate, since the mass of the final dehydration product is the same as the mass of the initial substrate (see Figure 2-1). However, it was observed that although these compounds do have the same mass, they have different retention times following separation over a reverse phase column and can be separated based on the time at which they elute from a C18 column. As it is possible to use LC/MS to detect both the disappearance of substrate and appearance of product for the reaction of EreA and EreB, this technique could be used to successfully monitor Ere activity in a stopped assay. In this approach, enzyme was left to react with substrate for a given amount of time, before the reaction was stopped, and the resulting products analyzed. The addition of three volumes of cold acetonitrile was the selected method used to stop the enzyme reactions, as suggested by Kim *et al.* (25).

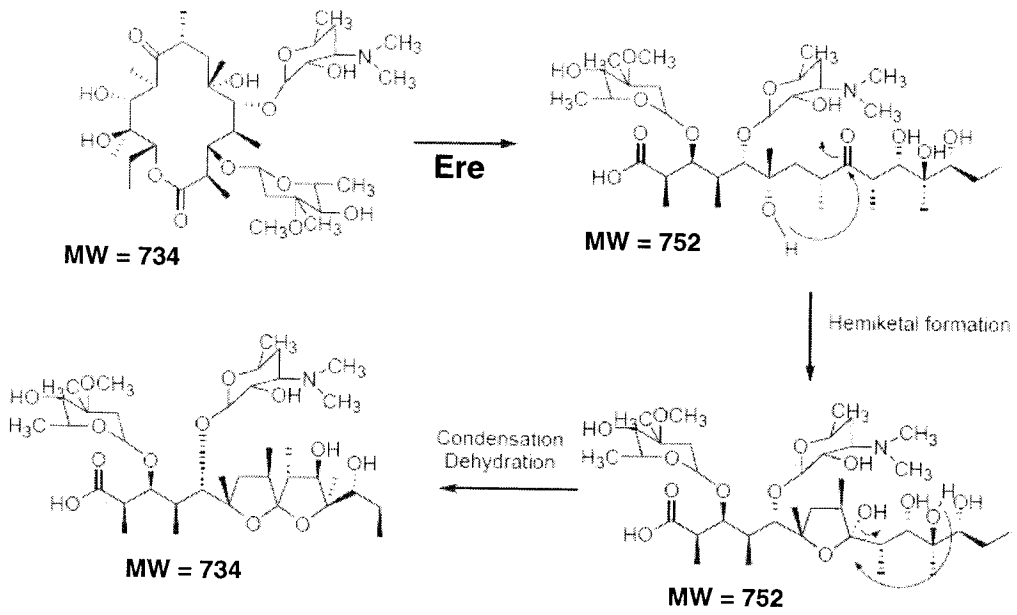

Figure 2-1. Proposed reaction carried out by EreA and EreB with subsequent non-enzymatic steps as originally proposed by Barthelemy *et al.* (8) Figure adapted from (50).

In order to use this method for a working enzyme assay, it was first necessary to determine appropriate concentrations of both erythromycin and EreB such that the signal for each compound of interest was detectable, but also reproducible between different replicates. Erythromycin concentrations of 1000 μM, 500 μM, 250 μM, 125 μM, 50 μM, 25 μM, and 5 μM were tried and it was determined that a concentration at or below 25 μM in the final sample after addition of acetonitrile was necessary to ensure reproducible signal intensities between sample replicates. The next step was to determine the range of time over which the progress curves for the reaction displayed linearity with respect to time, and an appropriate concentration of EreB. To do this, 0.15 μg or 0.075 μg EreB was incubated with 25 μM erythromycin in a 50 μL reaction. The reaction was allowed to proceed for 2, 5, 10, and 20 minutes before each reaction was stopped with three volumes of acetonitrile, and precipitated protein spun down with a microcentrifuge. A no

enzyme control was included as a zero time-point, and each reaction was performed in duplicate. LC/MS was then used to detect the compounds of interest, and the intensities of the appropriate mass peaks were plotted against time to obtain progress curves for each reaction.

2.2.8.2. Thin-layer Chromatography with [^{14}C]erythromycin

Radiolabelled erythromycin was used in combination with thin-layer chromatography in order to detect products and reactants of the reaction catalyzed by erythromycin esterases. As with the LC/MS assay, a stopped assay approach was used. In each reaction, 100 μM erythromycin containing 4.0 x 10^{-3} μCi [^{14}C]erythromycin (Perkin Elmer, Boston) was incubated with 0.75 μg EreB for 1 hour, and the reaction was stopped with the addition of 50% methanol. Control reactions without enzyme were included for each reaction. Any precipitated protein was removed by centrifugation and 5 μL of each reaction was applied on a silica gel plate. The plate was developed for 10 minutes in a pre-equilibrated TLC chamber using 100% methanol as the solvent system. Once the plate was removed from the chamber, dried, and wrapped in cellophane, it was exposed to a phosphor-storage imaging screen (GE Healthcare) for 35 minutes, and the resulting image was captured with the use of a Typhoon™ variable mode imager. ImageQuant 5.2 software was used to quantify relative radioactive intensity, and the corresponding amount of [^{14}C]erythromycin present per spot was calculated based on a standard curve generated from the erythromycin alone (no enzyme) controls.

Optimization of this assay was performed using unlabelled substrate. For detection of erythromycin, plates were sprayed with 10% H_2SO_4 in ethanol and then heated at 100 °C for 15 minutes as described by Courvalin (7). This allowed for the

visualization of substrate and product on the developed plate, but was not an approach amenable to quantification of substrate. Initially, 100% methanol had been used as the solvent system, but other solvent systems were investigated in order to optimize separation of products and substrate, including varying ratios of chloroform:methanol, and 19:6:75 methanol:actetone:water. Finally, 50:50 chloroform:methanol was selected as the best solvent system. The amount of time the plate was developed was also optimized, and times between 35 minutes, and 20 hours were investigated. It was found that the optimal duration of plate development was about 16 hours. The linear range in a progress curve of decrease in erythromycin spot intensity over time was determined, by incubating enzyme with substrate for 1, 2, 5, 10, 20 and 30 minutes. It was found that the progress curves exhibited a linear range for the first 20 minutes, and kinetic values were then obtained using varying substrate concentrations from 12.5 – 500 μM. After plate development and quantification, Grafit software 4.0.21 (Erithacus software) (26)was used to determine Michealis-Menten kinetics, with initial rates determined using Equation 1 and the non-linear least squares method.

$$v = (k_{cat}/E_t)[S]/(K_m + [S]) \quad [1]$$

v = initial reaction velocity
k_{cat} = turnover number
S = substrate concentration
K_m = substrate concentration at half maximum velocity
E_t = total enzyme amount present in each reaction

2.2.8.3. Spectrophotometric assay with *p*-nitrophenyl butyrate

A number of commercially available chromogenic esterase substrates exist, and if these could be utilized as substrates by the Ere proteins, would allow for the development of a continuous assay. Advantages of a continuous assay would be the ease and speed at

which such an assay could be performed, the ability to run several experiments in parallel simultaneously, and the immediate identification of problems. The following substrates were purchased from Sigma-Aldrich: p-nitrophenyl acetate (*p*-NPA), *p*-nitrophenyl butyrate (*p*-NPB), *p*-nitrophenyl valerate (*p*-NPV), *p*-nitrophenyl decanoate (*p*-NPD), *p*-nitrophenyl laurate (*p*-NPL), and *p*-nitrophenyl myristate (*p*-NPM) (see Figure 2-3). These esterase substrates, when hydrolysed, release the product *p*-nitrophenol, which is bright yellow in colour and has a characteristic absorbance wavelength of 405 nm (see Figure 2-2).

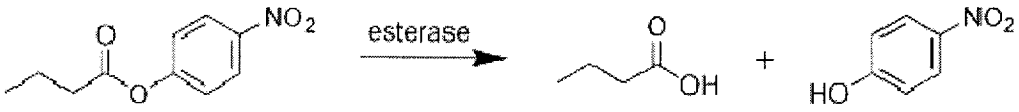

Figure 2-2. Sample reaction of hydrolysis of esterase substrate, *p*-nitrophenyl butyrate

The ability of EreA and EreB to act on these substrates was examined with assay conditions initially developed for the examination of environmentally isolated cutinase enzymes (20). This method was adapted for reaction volumes of 250 µL in a 96-well plate from the original 1 mL cuvette format. Each 250 µL reaction contained 50 mM sodium phosphate buffer pH 7.0, 0.2% Triton X-100 to aid with solubilization of substrate, and 2.3 mM *p*-NPX. Reactions were initiated by addition of enzyme.

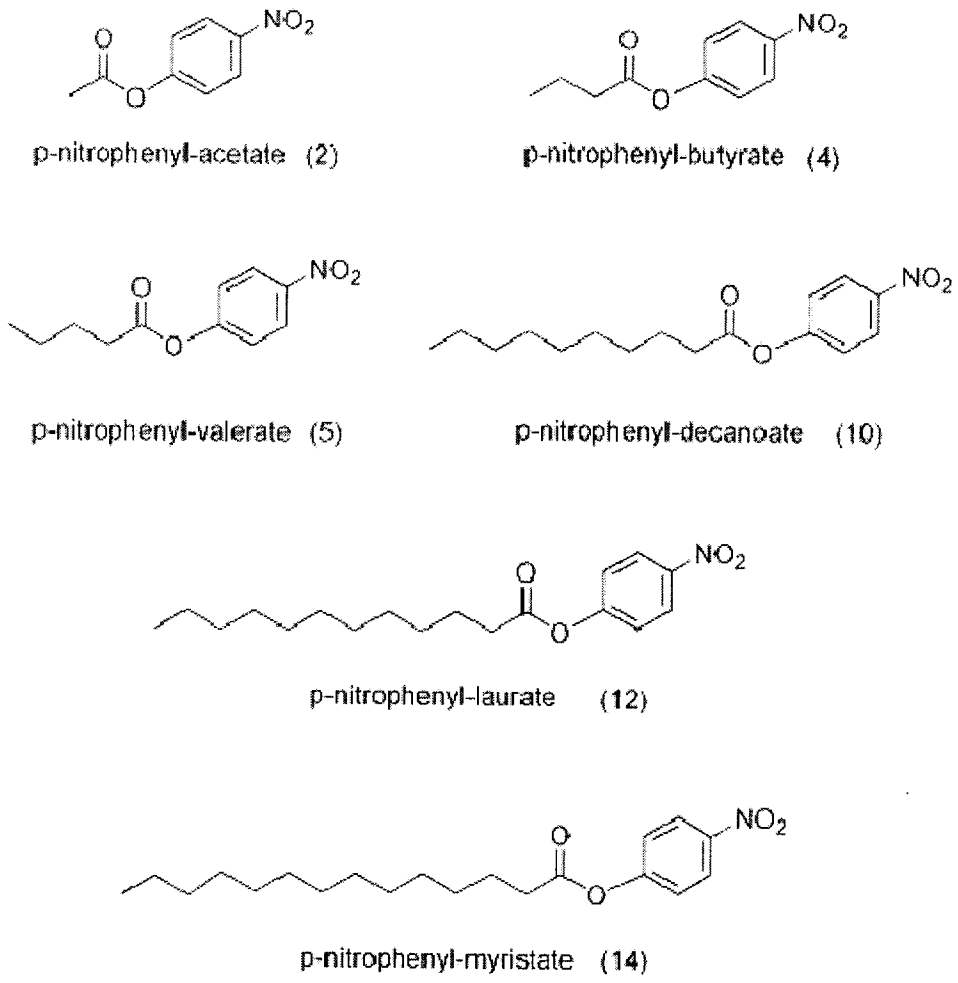

Figure 2-3. Commercially available chromogenic esterase substrates used in this study

In the optimized assay, esterase activity was measured with *p*-nitrophenyl butyrate (*p*-NPB) as the substrate. Each 250 µL reaction mixture contained 50 mM HEPES pH 7.5, 0.2 % Triton X-100 (Sigma), 0.02 mg purified erythromycin esterase protein, and 15.6 – 2000 µM *p*-NPB. Reactions were monitored at 405 nm for 45 minutes, during which a linear relationship was observed. The amount of reaction product released (*p*-nitrophenol) was calculated based on a prepared standard curve of *p*-nitrophenol in assay buffer. As with the [^{14}C]erythromycin TLC method, Grafit software

4.0.21 (Erithacus software) (26) was used to determine kinetic parameters, with initial rates determined using Equation 1 and the non-linear least squares method.

2.3. Results

2.3.1. Gene Amplification and Plasmid Construction

PCR was successfully used to amplify the predicted esterase genes from *P. stuartii* , *E. coli*, *S. erythraea* and *S. coelicolor*. Following recombination into Gateway vector pDONR 201, sequencing was performed to ensure the correct gene was present. Recombination into either pDEST14 (no tag), pDEST15 (N-terminal GST tag), pDEST17 (N-terminal His tag), or pDEST42 (C-terminal His tag) was achieved and resulting constructs were tested for protein expression and solubility. In the case of *ere*-bc, the gene was successfully re-ligated into pET28a using *Nde* I and *Xho* I restriction sites to allow for expression of N-terminally hexa-His tagged protein and the possibility of tag removal through thrombin cleavage.

2.3.2. Protein Solubility Assays

Expression constructs were tested for protein solubility and it was found that the amount of protein expressed and the protein solubility varied, depending on the presence of a His or GST tag. Table 2-3 shows all constructs created in-house, or donated (in the case of *ere*-bc in pET21b) and the resulting expression and solubility of the proteins under investigation. For both EreA and EreB, the presence of a His-tag, either at the C-terminal or N-terminal end led to very poor protein solubility. This was overcome by the use of pDEST14, an expression vector allowing for expression of native un-tagged protein. Ere-se was slightly soluble with expression using both pDEST17 and pDEST14,

however a greater level of expression with pDEST14 lead to its selection as an appropriate vector.

Table 2-3. A summary of results from solubility and disc diffusion assays with existing *ere* constructs transformed into *E. coli* BL21 (DE3) cells. S indicates the presence of Ere protein in the soluble fraction after cells are lysed, while I indicates the absence of soluble protein. + indicates the ability of cells to grow in the presence of 250 μg/mL erythromycin and 1mM IPTG, while – indicates susceptibility to 250 μg/mL erythromycin.

	N-term His tag		**C-term His tag**			**Native protein**		**N-term GST**
	pDEST17	pET28a	pET DEST42	pET22b	pET21b	pDEST14	pET22b	pDEST15
ereA	I/+		I/-			S/+		
ereB	I/+		I/-	I/-		S/+		I/+
ere-sc	I/-	I/-					I/-	
ere-se	S/-					S/-		
ere-bc		S/-			S/-			
Empty vector		-		-			-	

As can be seen from the Table 2-3, some additional cloning was done to move some of these genes in to pET vectors (pET28a, pET22b) in order to test solubility using an alternative expression system. In the end, pDEST14 was selected as an appropriate vector for the expression and purification of EreA from *P. stuartii* and EreB from *E. coli.* pDEST14 was also selected as appropriate vector for the putative esterase from *S. erythraea.* Both pET21b and pET28a were used for the expression and purification of Ere-bc.

A sample solubility assay for native, untagged EreB is shown below in Figure 2-4. It can be seen that soluble protein is found in the lane containing protein expressed after overnight growth at 16°C.

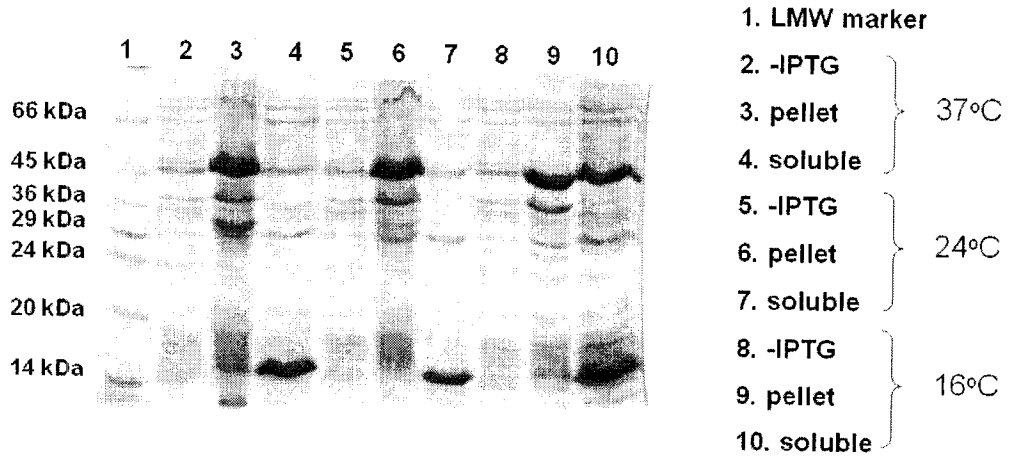

Figure 2-4. Solubility assay for native *E. coli* EreB. Protein was expressed in *E. coli* BL21 (DE3) cells induced with 1mM IPTG, and grown for 10 hours at 16°C, 5 hours at 24°C or 3 hours at 37°C. Soluble EreB is visible in Lane 10.

It was interesting to note that the C-terminally tagged constructs for EreA and EreB did not yield functional protein, as determined by the inability of cells expressing this protein to grow in the presence of erythromycin. Possibly the C-terminal tag interferes with correct folding or activity. Although the C-terminal His tagged construct for Ere-bc resulted in a high level of expression and soluble protein, expression of this protein was not able to confer resistance to otherwise susceptible cells. Knowing that the C-terminal constructs for EreA and EreB were also unable to confer resistance, this suggested the C-terminal tag may interfere with the activity of against erythromycin as well. To address this potential problem, Ere-bc was additionally ligated into pET28a (+) encoding for an N-terminal tag that could be cleaved with the use of thrombin. It was found that substitution of the C-terminal His tag for an N-terminal tag did not introduce the ability of cells expressing Ere-bc to grow in the presence of erythromycin, indicating that the C-terminal tag alone is not responsible for the lack of activity, and instead the protein itself may not be an active erythromycin esterase.

2.3.3. Purification of known and putative erythromycin esterases

Ere proteins were successfully purified using the chromatography steps described above (See Figure 2-5). All had apparent molecular weights by SDS-PAGE corresponding to predicted molecular weight by primary sequence. From one litre of culture, an average yield for EreA was about 20 mg, for EreB 14 mg, for Ere-bc 80 mg, and for Ere-se about 6 mg.

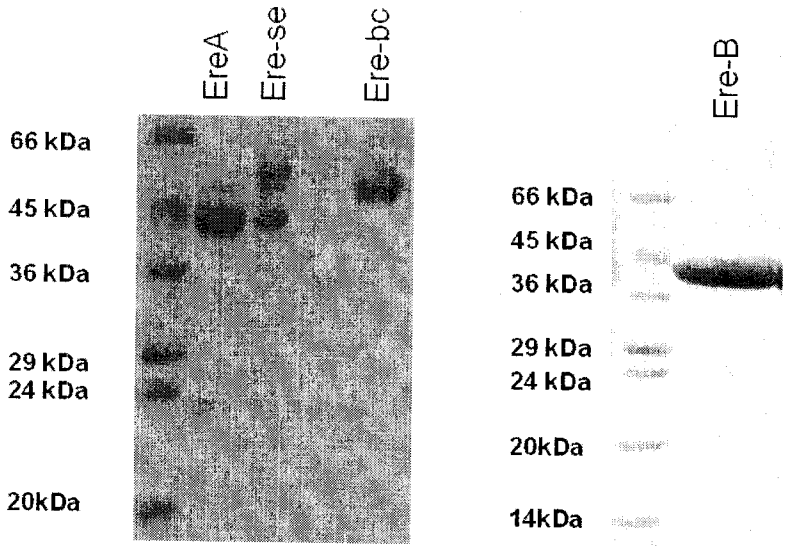

Figure 2-5. Purified erythromycin esterases EreA, Ere-se, Ere-bc, EreB.

Table 2-4. Summary of average purification yields and predicted and observed molecular weights from purified esterases

Protein	Predicted Molecular Weight (kDa)	Observed Molecular Weight by SDS-PAGE (kDa)	Average Purified Protein Yield (mg/L)
EreA	44.7	40	20
EreB	48 .2	42	14
Ere-se	42.2	40	6
Ere-bc	50.5	54	80

2.3.4. Minimum inhibitory concentrations of erythromycin against cells expressing *ere* genes

E. coli cells expressing each of the different expression constructs for the erythromycin esterases were tested for their ability to grow in the presence of erythromycin. Cells expressing EreA and EreB showed increased MIC values when compared to the empty vector control (see Table 2-5). It was found that these increased MIC's (>1mg/ml and >2 mg/ml for EreA and EreB respectively) were consistent with the ability of these proteins, when purified, to inactivate erythromycin and other macrolides. In contrast, the putative erythromycin esterases from *S. erythraea* and *B. cereus* did not appear to confer erythromycin resistance when expressed in *E. coli*, as there was no change in MIC value when compared to the control. Again, there was a correlation with the inability of these proteins when purified to inactivate erythromycin and other macrolides. Finally, the putative esterase from *S. coelicolor* was not found to increase MIC value when expressed.

Table 2-5. MIC's of erythromycin against *E. coli* BL21 (DE3) harbouring *ere*'s from different source organisms

Ere and plasmid vector	MIC µg/ml
pDEST14-EreA	1024
pDEST14-EreB	>2048
pDEST14-Ere-se	64
pET22b(+)-Ere-sc	64
pET21b(+)-Ere-bc	64
pET28a(+)	64

2.3.5. Activity of purified erythromycin esterases

Purified EreA and EreB were both seen to inactivate erythromycin as determined by simple disc diffusion bioassay. However, a slightly different profile of substrate specificity was seen for the two enzymes. EreB was able to inactivate all macrolides in our panel with the exception of the ketolide telithromycin. This is possibly due to the long carbamate extension on telithromycin which may hinder the ability of this antibiotic to get to the active site of the enzyme. It is also possible that the absence of the cladinose sugar does not allow the enzyme to recognize this semi-synthetic substrate. EreA, in addition to being unable to inactivate telithromycin, was also seen to have no activity against the semi-synthetic drug azithromycin (see Figure 2-6 for a sample bioassay using EreA). None of the other purified putative erythromycin esterases were shown to inactivate any of the macrolides tested here. A summary of the substrate specificity of the erythromycin esterases in this study is shown in Table 2-6.

Table 2-6. Activity of purified Ere enzymes against panel of macrolides. + indicates ability to completely inactivate a 50 μL reaction of 100 μM antibiotic after 1 hr of incubation with 0.08 mg purified protein, as determined by Kirby-Bauer disc diffusion assay

Ere	erythromycin	azithromycin	clarithromycin	roxithromycin	telithromycin
EreA	+	-	+	+	-
EreB	+	+	+	+	-
Ere-se	-	-	-	-	-
Ere-bc	-	-	-	-	-

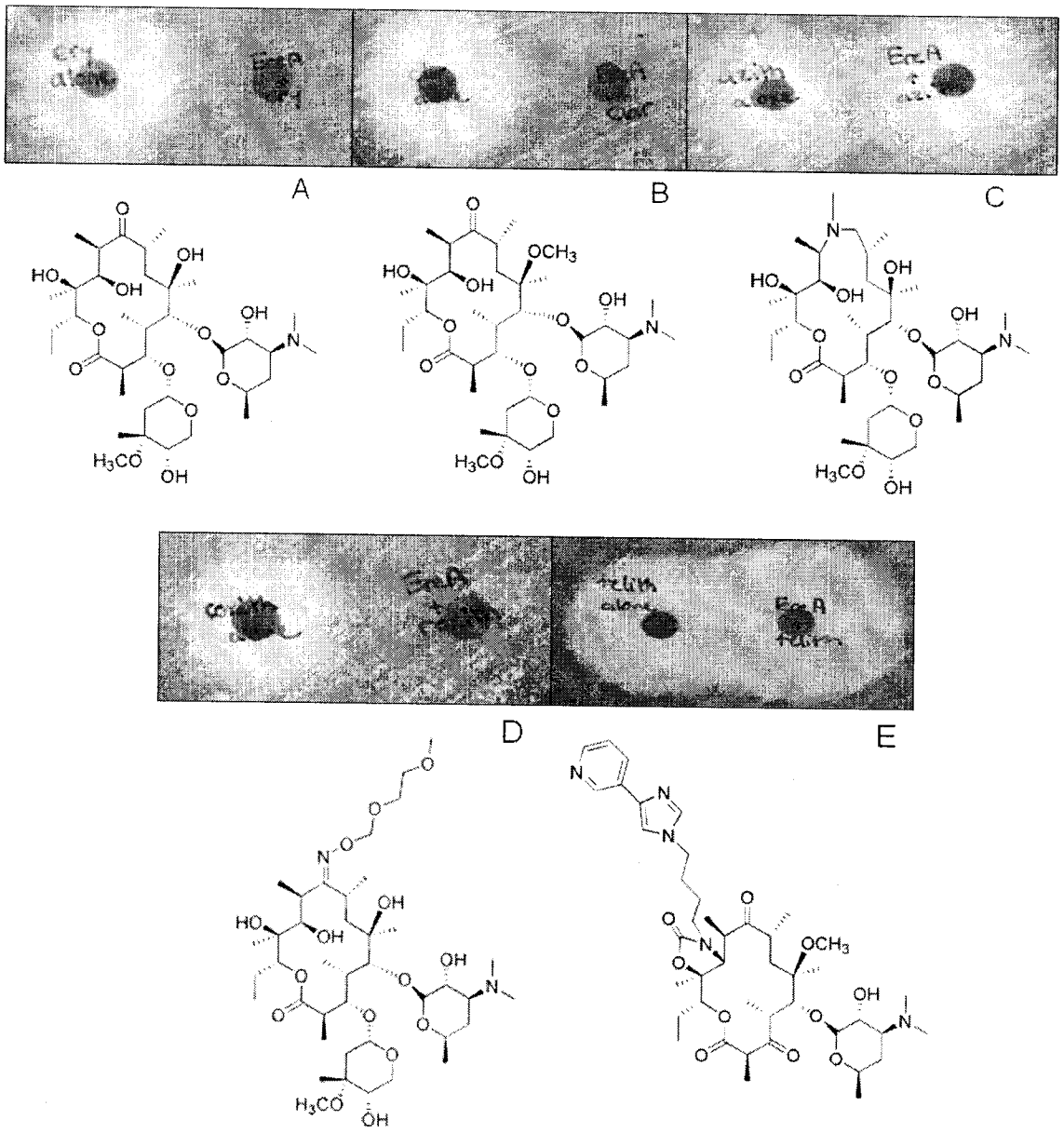

Figure 2-6. Activity of purified EreA against erythromycin and other semi-synthetic macrolides as determined by loss of antimicrobial activity against the indicator organism *M. luteus*. Antibiotics incubated for 1 hour with 0.08 mg EreA. Structures of the antibiotics are shown below: A. erythromycin, B. clarithromycin, C. azithromycin, D. roxithromycin, E. telithromycin.

2.3.6. Products of reaction analyzed by liquid chromatography mass spectrometry

The products of macrolide inactivation by EreA and EreB were analyzed by LC/MS to confirm that the loss of antimicrobial activity seen in the bioassay was the

result of inactivation of erythromycin through hydrolysis, as expected. Recall the predicted product from an enzymatic hydrolysis of erythromycin would have an increase in mass of 18 amu due to the addition of water across the ester bond (see Figure 2-1). This first step is followed by subsequent non-enzymatic reactions leading to a final product with a mass of 734 amu, identical to that of erythromycin, the starting material. It was of interest to us to see if the final dehydration product, showed any shift in retention time when eluting from a C-18 column, in order to help us distinguish between the starting substrate and final product. A shift in retention time was observed, as seen below in Figure 2-7.

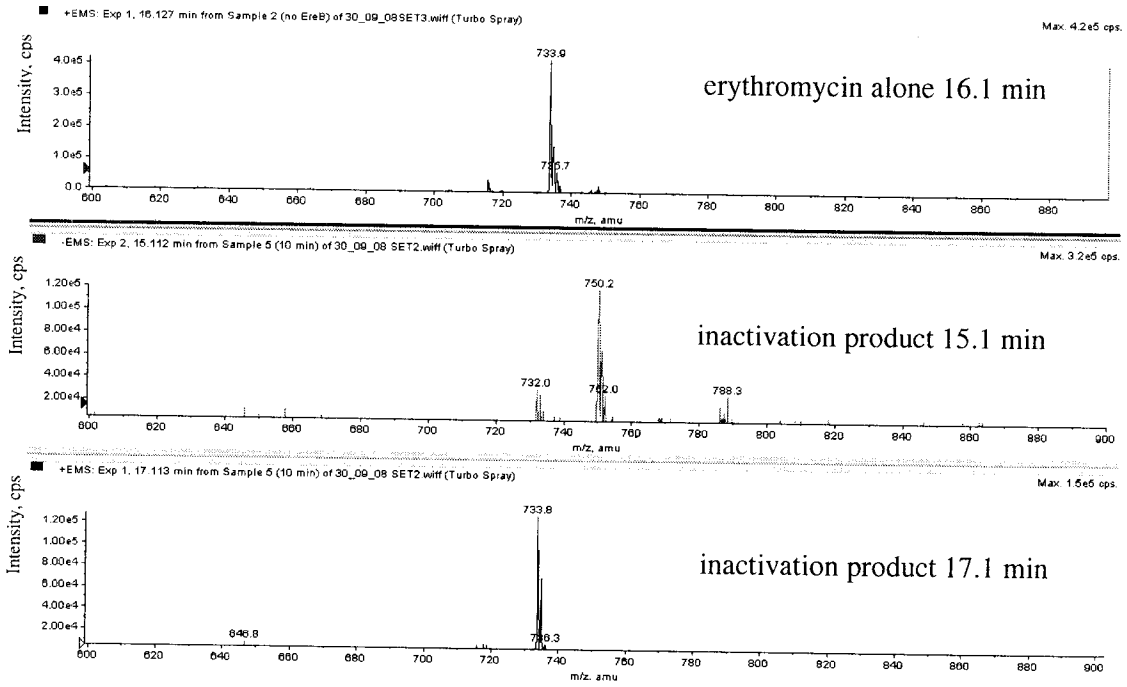

Figure 2-7. LC/MS analysis for intact and hydrolyzed erythromycin. Top panel shows erythromycin alone, lower panels show reaction products of erythromycin with EreB.

Table 2-7. Expected and observed products from 3 hour incubations of 0.1 mg/mL EreA or EreB with 25 μg/mL erythromycin as detected by LC/MS

Reaction	Expected *m/z* (amu)	Observed *m/z* (amu) +EMS	-EMS
erythromycin alone	734	733.9 (15.6 min)	-
erythromycin + EreB	752 (hydrolysis product) or (hemiketal)	751.6	750.2
	734 (final dehydration product)	733.8 (17.1 min)	732.0
erythromycin + EreA	752 (hydrolysis product) or (hemiketal)	751.4	750.2
	734 (final dehydration product)	734.0 (17.1 min)	732.2

In our analysis, masses corresponding to all expected products in the inactivation of erythromycin were detected. The expected products and the actual products detected with LC/MS in the reactions of erythromycin with the erythromycin esterases are summarized in Table 2-7.

With reactions catalyzed by EreB, there was a clear difference between the retention time of 15.6 minutes for a mass-to charge ratio (*m/z*) of about 734 for erythromycin in the absence of enzyme, and a retention time of 17.1 minutes for a *m/z* of about 734 in the presence of enzyme. It can also be seen that these two compounds having the same mass but eluting at different times, appear to ionize differently, with negative ions having a *m/z* of about 734 only being detected in the sample incubated with enzyme (see Figure 2-7). It was therefore assumed that the species with a retention time

of 17.1 minutes and a mass-to-charge ratio of about 734 corresponded to the final dehydration product, while the species with a retention time of 15.6 minutes and the same mass corresponded to unhydrolyzed erythromycin.

It was expected that EreA and EreB would yield identical products when the reactions were eluted from a C-18 column and detected with mass spectrometry, and this was indeed the case. Like with EreB, there was a clear difference between the retention time of 15.6 minutes for a mass-to charge ratio (*m/z*) of about 734 for erythromycin alone, and a retention time of 17.1 minutes for a *m/z* of about 734 in the presence of enzyme, corresponding to the final dehydration product. As with EreB, an additional peak at a retention time of 15.1 minutes with a *m/z* of -750 was observed, corresponding to the expected intermediate product. By mass spectrometry analysis, the products of the reactions catalyzed by the two enzymes are indistinguishable.

Clarithromycin, because of its methoxy group at C6, is not expected to undergo the subsequent non-enzymatic steps after hydrolysis that occur with erythromycin. The reaction products of clarithromycin with EreB were also examined by LC/MS to confirm that the inactivation product was as expected, the result of hydrolysis by an Ere. The expected and observed products in a reaction of EreB with clarithromycin are summarized in Table 2-8.

Again, for the reaction of clarithromycin with EreB, a compound with a mass corresponding to the expected hydrolysis product of clarithromycin appears. The presence of an additional compound with a mass of 748.2 even after three hours of incubation with EreB indicates that the hydrolysis of clarithromycin was likely incomplete. Perhaps this is because clarithromycin is not the preferred substrate for EreB.

This is the first time, to our knowledge, that the products of inactivation of clarithromycin by any erythromycin esterase, or the inactivation products of erythromycin by a purified EreB have been examined.

Table 2-8. Expected and observed products from 3 hour incubations of 0.1 mg/mL EreB with 25 μg/mL clarithromycin as detected by LC/MS

Reaction	Expected *m/z* (amu)	Observed *m/z* (amu) +EMS	-EMS
clarithromycin alone	748	748.1	-
clarithromycin + EreB	766	765.8 748.2	764.2

In the inactivation studies, it was found that both EreA and EreB were capable of inactivating roxithromycin, the structure of which is shown in Figure 2-6 (D). In order to determine if the inactivation of roxithromycin was simply due to removal of the extension at C-9, and subsequent reversion to erythromycin, inactivation product from a reaction of EreB with roxithromycin was examined by mass spectrometry. If the expected mass corresponded to roxithromycin (MW = 837 alone, MW = 855 after hydrolysis), this would indicate that roxithromycin was truly being used as a substrate by EreB, while if any erythromycin was observed, this would suggest that in actuality it was erythromycin being inactivated. It was found that inactivation was due to hydrolysis of roxithromycin, with a product having a mass to charge ratio of 855 appearing upon incubation with EreB, and no mass corresponding to erythromycin (MW = 734) was observed either with roxithromycin alone, or roxithromycin with EreB. Therefore, inactivation of roxithromycin was due to ring hydrolysis of this antibiotic, rather than reversion to erythromycin and subsequent inactivation of erythromycin.

Due to the lack of sensitivity in the disc diffusion bioassay, mass spectrometry was additionally used to search for any reaction products undetectable by inactivation assay for the other erythromycin esterases (Ere-se and Ere-bc). Reactions containing 25 μg erythromycin were incubated for 3, 16 and 24 hours with up to Ere-se, and Ere-bc, but no breakdown products of erythromycin were detected by this method, confirming that these enzymes are unable to hydrolyze erythromycin under these conditions.

2.7. Assay development and Steady State Kinetic parameters

2.7.1. Development of LC/MS assay

Some optimization of this method for use as a quantitative assay was performed. A detection limit of <25 μM was established for this method. It was found that concentrations above this amount of substrate after addition of acetonitrile were not reproducible. With EreB, it was determined that the initial linear range of reaction was within 2-5 minutes, as shown below in Figure 2-8. The ability of LC/MS to investigate reactions of erythromycin esterases with various substrates, as well as the sensitivity of the detection method (which means only very small amounts of both enzyme and antibiotic need be used in each reaction), are practical advantages to using this method.

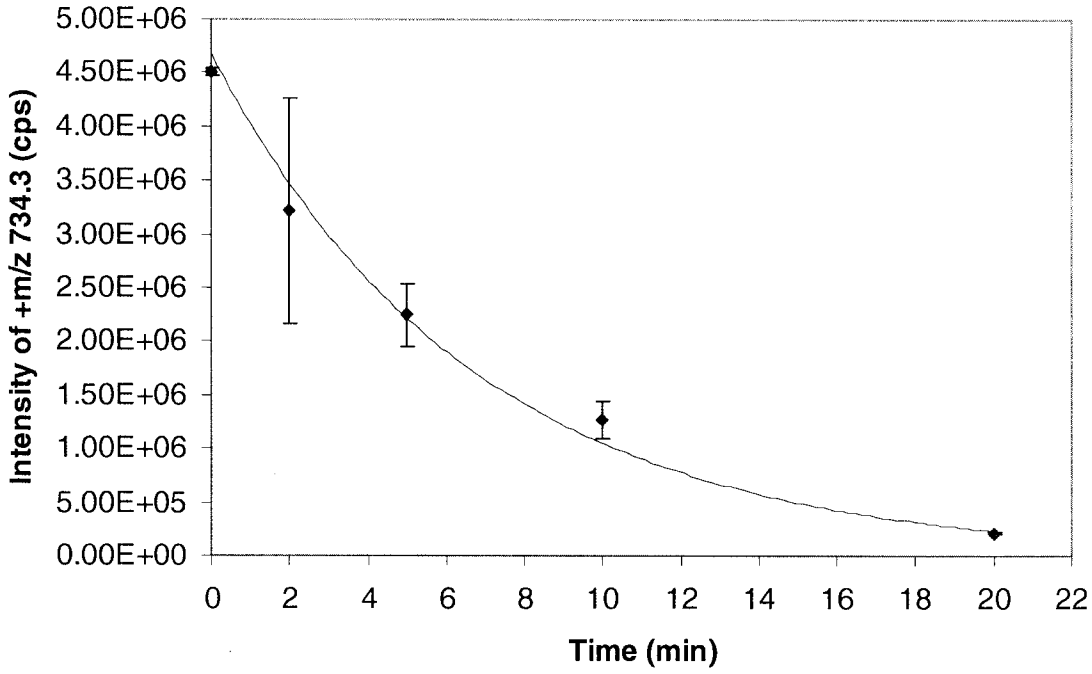

Figure 2-8. Sample progress curve for the disappearance of erythromycin over time in a 50 µL reaction of 0.15 µg EreB with 100 µM erythromycin as detected by LC/MS.

2.3.7.2. [^{14}C]erythromycin and Thin-layer Chromatography

A successful separation of substrates and products was achieved through the use of TLC, as shown below in Figure 2-9. Although initially, a solvent system of 100% methanol did allow for quick separation between products and reactants, there was some overlap of radioactive signal once the plates were imaged. After experimenting with various solvent systems, it was found that a solvent system of 50:50 chloroform:methanol allowed for the best separation of products and reactants.

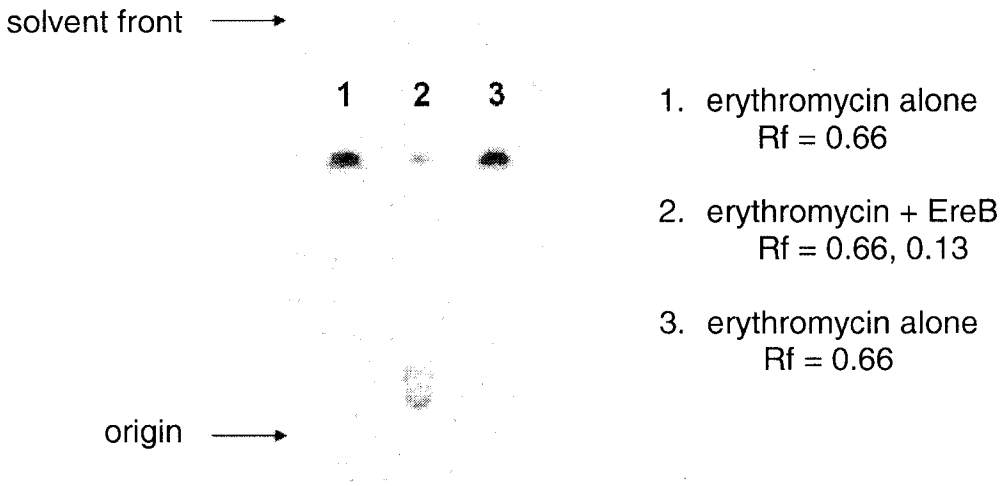

Figure 2-9. Phosphor image of erythromycin and EreB inactivated erythromycin, as separated on a silica gel plate with 50:50 methanol:chloroform as the solvent system. Reaction of 100 μM erythromycin (containing 4.0 x 10^{-3} μCi [^{14}C]erythromycin) was incubated with 0.75 μg EreB in a 50 μL reaction for 20 minutes.

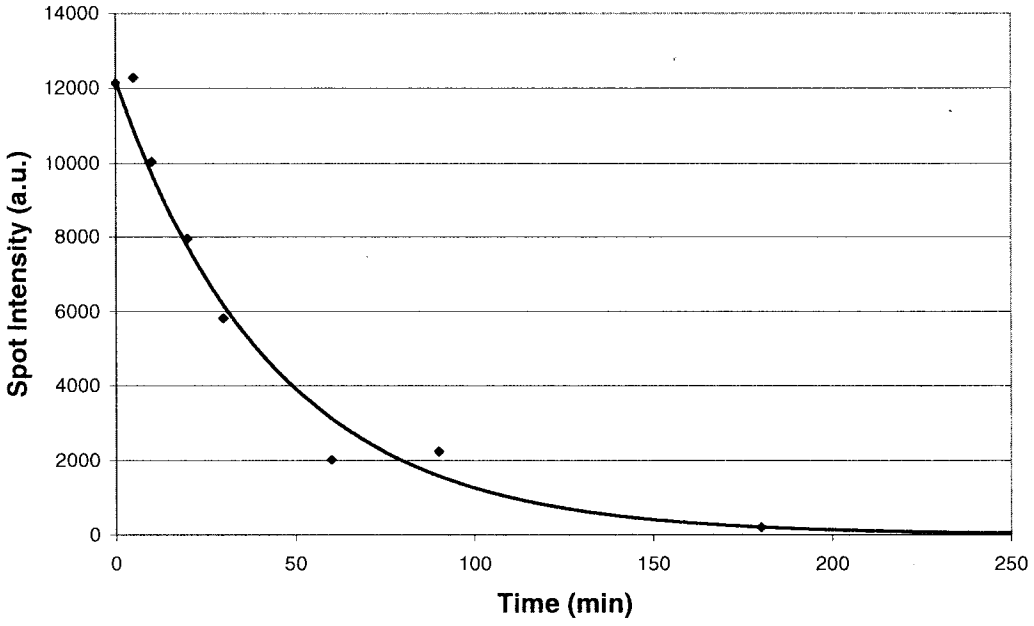

Figure 2-10. Sample progress curve for the disappearance of [^{14}C]erythromycin over time in a 50 μL reaction of 0.75 μg EreB with 100 μM erythromycin. Intensity of [^{14}C]erythromycin signals were quantified with ImageQuant 5.2 software.

Once the initial conditions for the separation of products and reactants had been obtained, the next step was to determine the range of time over which the progress curves for the reaction displayed linearity, and an appropriate concentration of EreB to use in each reaction. Figure 2-10 shows a sample progress curve following the disappearance of erythromycin over time, and over the first 30 minutes, the progress curve does appear to be linear. Based on this information, a final time point of 20 minutes, and a range of 12.5 μM – 200 μM erythromycin was selected as conditions for the enzymatic assay. Instead of stopping the reactions with methanol, it was found that the use of 5% trichloroacetic acid (TCA) gave more consistent relative intensities between replicate spots. These conditions were used to determine kinetic parameters for EreB with erythromycin, and these values are shown in Table 2-9. Problems with reproducibility lead to difficulty in repeating these results with the same enzyme preparation at a later date, and with subsequent enzyme preparations. Despite repeated attempts to re-optimize this assay with fresh enzyme preparations, the range of time over which the progress curves for the reaction displayed linearity was not found. The continuous assay utilizing a commercially available esterase substrate was therefore used for the remainder of the kinetic analysis.

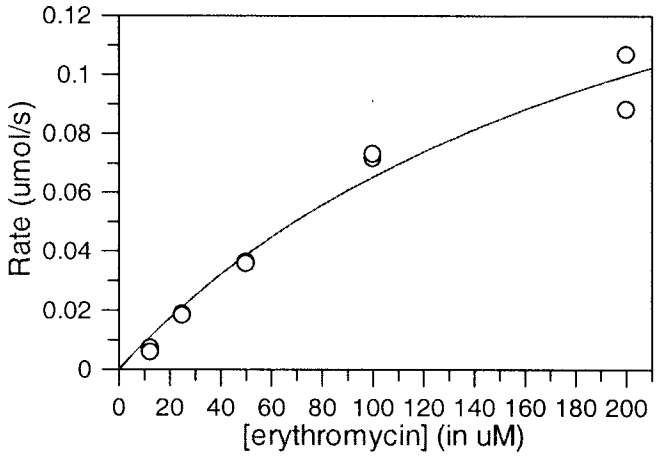

Figure 2-11. Michaelis-Menten curve for determination of steady-state kinetic data for EreB with erythromycin

Table 2-9. Steady state kinetic parameters for EreB as determined by thin-layer chromatography assay

Enzyme	K_m, mM	k_{cat}, s^{-1}	k_{cat}/K_m, $s^{-1}M^{-1}$
EreB	0.224	1.33×10^4	5.93×10^7

2.3.7.3. Continuous Assay with *p*-nitrophenyl butyrate as Esterase Substratetttt

Of the different p-nitrophenyl esterase substrates, it was found that *p*-nitrophenyl butyrate was a good substrate for both EreA and EreB. Although both *p*-NPA and *p*-NPV could also be utilized by these enzymes, non-enzymatic hydrolysis of *p*-NPA lead to very high background readings. Although non-enzymatic hydrolysis was not a problem for *p*-NPV, rates of reaction for this substrate were slower than those for *p*-NPB, and the difference between non-enzymatic hydrolysis and enzyme catalyzed hydrolysis was almost indistinguishable for low substrate concentrations. *p*-NPB was therefore selected for further optimization in a continuous 96-well plate format. Once initial assay conditions had been established, it was necessary to determine the linear range of the reaction, where the progress curve was linear with respect to time. It was determined that progress curves remained linear for the first 20-40 minutes of the reaction. A sample progress curve for the reaction of *p*-NPB with EreA is shown below in Figure 2-12. Although some non-enzymatic hydrolysis is seen over time, this can be corrected for by subtracting the no-enzyme control values from the progress curve for enzyme catalyzed hydrolysis.

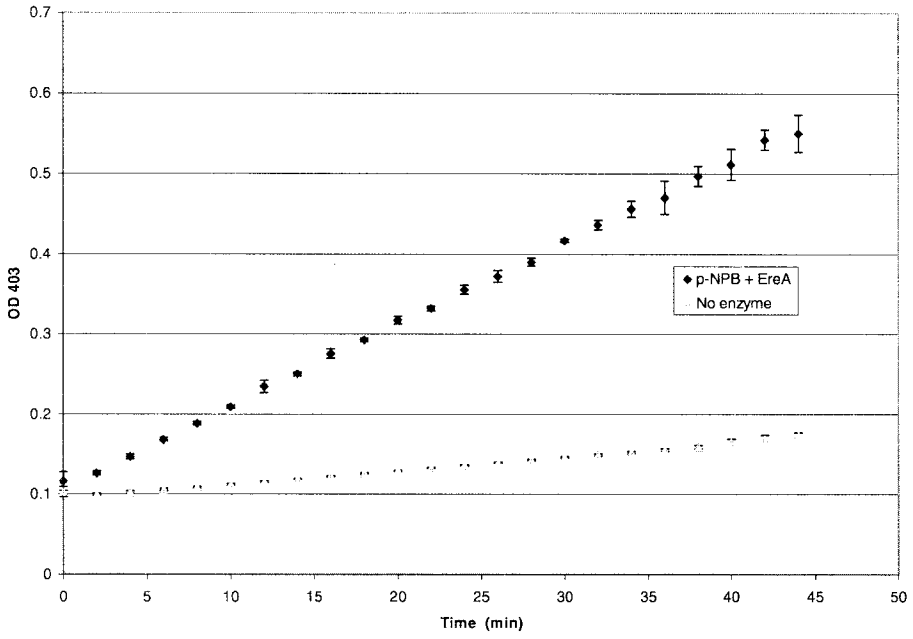

Figure 2-12. Sample progress curve for the release of *p*-nitrophenol over time in 250 µL reactions of 0.02 mg EreB (or no enzyme control) with 2.3 mM *p*-nitrophenyl butyrate. Reactions were performed in triplicate, and initiated by addition of enzyme.

In order to determine steady-state kinetic values for the erythromycin esterases using this substrate, reactions were set up containing between 3.9 µM and 2 mM *p*-NPB and the initial rates over 20 minutes were determined. Sample Michaelis-Menten curves for the each of the esterases are shown in Figure 2-13, and kinetic parameters for EreA, EreB, Ere-se, and Ere-bc are summarized below in Table 2-10. When compared to the kinetic values obtained for EreB using the [^{14}C]erythromycin TLC assay, it can be seen that there is a marked increase in catalytic efficiency (k_{cat}/K_m) with the natural substrate erythromycin (5.93 x 10^7 $s^{-1}M^{-1}$) as opposed to *p*-NPB (6.09 x 10^4 $s^{-1}M^{-1}$), although the K_m values for the two substrates are comparable (0.224 mM for erythromycin and 0.281 mM for *p*-NPB). Using *p*-NPB and comparing EreA with EreB, the catalytic efficiency

(k_{cat}/K_m) of the two enzymes is very similar, at 9.03 x 10^4 $s^{-1}M^{-1}$ and 6.09 x 10^4 $s^{-1}M^{-1}$, although the turnover number (k_{cat}) for EreA is higher than that of EreB.

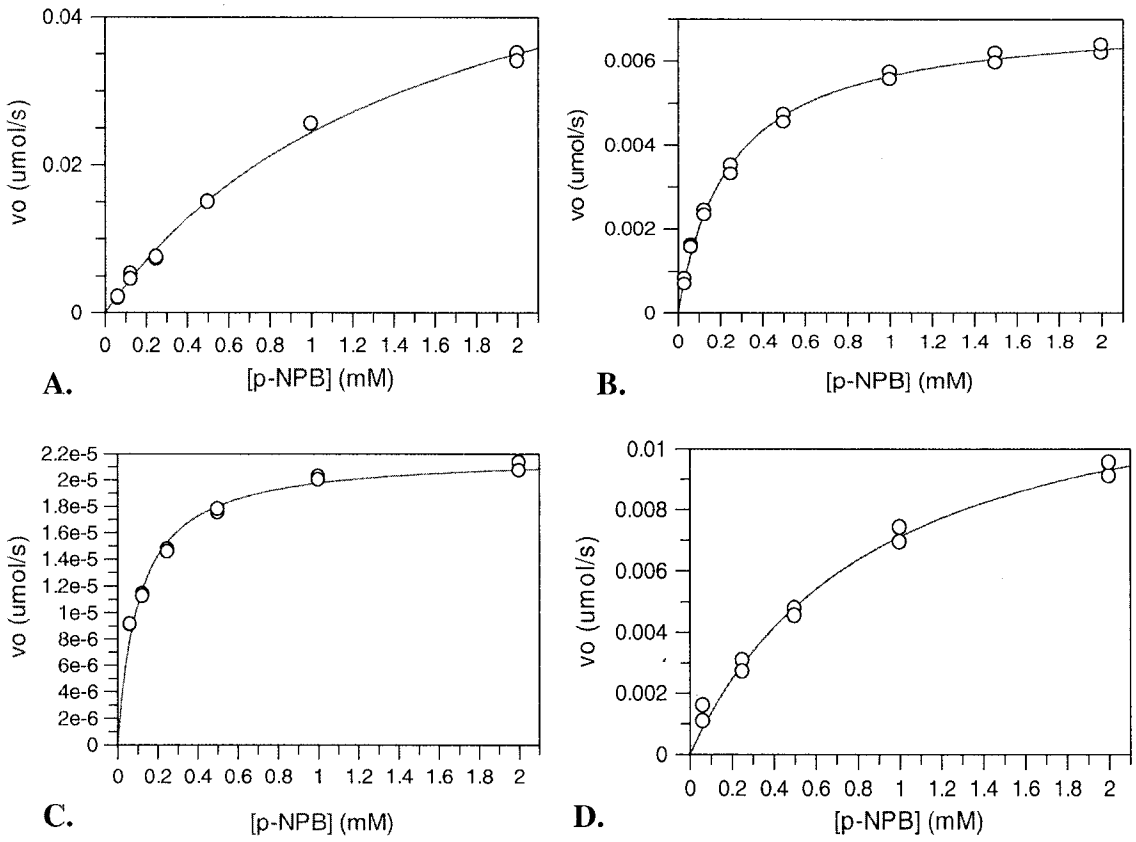

Figure 2-13. Michaelis-Menten curves for the determination of steady-state kinetic parameters for each of the esterase enzymes. A. EreA, B. EreB, C. Ere-se, D. Ere-bc.

Table 2-10. Steady state kinetic parameters of Ere enzymes, as determined with *p*-nitrophenyl butyrate as esterase substrate

Ere	K_m, mM	k_{cat}, s^{-1}	k_{cat}/K_m, $s^{-1}M^{-1}$
EreA	1.54 ± 0.15	139 ± 7.6	9.03 x 10^4
EreB	0.281 ± 0.012	17.1 ± 0.22	6.09 x 10^4
Ere-se	0.107 ± 0.008	0.046 ± 0.0009	4.30 x 10^2
Ere-bc	0.896 ± 0.11	34.1 ± 1.9	3.81 x 10^4

Interestingly, both Ere-se and Ere-bc were able to use *p*-NPB as a substrate, although they were unable to hydrolyze any of the macrolide antibiotics tested. These enzymes, then, are esterases, although their activity in this assay is less than that of EreA

and EreB, and they were not shown to be active macrolide antibiotic resistance proteins. Whether they could become enzymes capable of hydrolyzing erythromycin if a few key amino acids were exchanged for those present in the active Ere proteins EreA and EreB, is a matter which will be discussed further in Chapter 4.

2.4 Summary and conclusions

Problems of protein solubility for EreA and EreB were overcome with the use of the pDEST14 expression vector, allowing for expression of native un-tagged protein. These two proteins were successfully purified with a combination of anion exchange and hydrophobic interaction chromatography.

The erythromycin esterases EreA and EreB, from *P. stuartii* and *E. coli* respectively were shown to be active resistance proteins, capable of hydrolyzing erythromycin and other macrolides. The substrate specificity of the two enzymes was not identical, in that EreA was incapable of hydrolyzing azithromycin, whereas EreB was able to inactivate this semi-synthetic antibiotic. Neither enzyme could hydrolyze the ketolide telithromycin. Although the enzyme from the producing organism *S. erythraea* is annotated as an erythromycin esterase based on its sequence similarity to EreB, this protein was not found to possess the anticipated activity when purified. Additionally, the protein from *B. cereus* was unable to inactivate any of the macrolides tested. The products of macrolide inactivation by EreA and EreB were examined with the use of LC/MS, and as expected, confirmed inactivation through hydrolysis. This is the first time the inactivation products of a purified EreB enzyme have been examined.

A quantitative enzyme assay was developed using the general esterase substrate *p*-nitrophenyl butyrate and this used to determine steady-state kinetic parameters for

these erythromycin esterase enzymes. It was interesting to note that the putative esterases from *S. erythraea*, and from *B. cereus* were capable of hydrolyzing this esterase substrate, confirming that these proteins do possess esterase activity. It may be that their true function is hydrolysis of an alternate substrate.

Chapter 3 – Structural Insights and Modelling of EreB

3.1 Overview

The determination of protein structure can yield valuable insights that allow for better understanding of how a protein is able to carry out a particular function. The examination of the relationship between structure and function can give information about substrate binding, which amino acid residues are necessary for catalysis and details about enzyme mechanism. Although to date, no crystal structure exists for EreA or EreB, it may be possible to make some inferences about structure based on previously determined structures which may share a similar fold. A model was generated for EreB, based on the crystal structures of two proteins from *B. cereus*, Ere-bc (Bcr136, PDB 2qgm) and Bcr135 (PDB 3b55), both determined by the Northeast Structural Genomics Consortium and deposited in the PDB. Based on this model, a putative active site was proposed, and some residues that may be necessary for enzyme catalysis were selected for site-directed mutagenesis.

3.2 Materials and Methods

3.2.1 Analytical Gel Filtration

Gel filtration was performed with the use of a calibrated Superdex-200 10/300 GL column, in order to examine the oligomeric state of EreA and EreB. In this technique, the elution volume of a given protein of unknown size is compared to that of a set of known standards, allowing the size of an unknown protein in its native state to be determined. Calibration was performed using a Gel Filtration Molecular Marker Kit (Sigma), and 50 mM HEPES pH 7.5, 50 mM NaCl, 0.1 mM EDTA, 5% glycerol as the

buffer system. Sample volumes of 100 µL sample at a concentration of 3-4 mg/mL containing 5% glycerol were injected onto the column at a flow rate of 0.5 ml/min.

3.2.2. Crystallization Trials

With help from Dr. Alba Guarné, initial crystal screens were set up using the hanging drop-vapour diffusion method with some commercially available screens. For EreB, drops were set at 4°C with protein at 5mg/mL and 10 mg/mL, against a reservoir of 0.5 M ammonium sulfate. Classics (QIAGEN), Index (Hampton Research), Wizard I and II (Emerald Biosciences), and PEG/Ion (QIAGEN) screens were set. Additionally, some crystals screens were set using the commercially available Wizard I and Wizard II sparse matrix screens, and EreA protein at 5mg/mL. Again, the hanging drop vapour diffusion method was used, and drops were set at both 4°C and 24°C.

In order to screen a broader range of crystallization conditions in a timely manner, purified EreB protein was also sent to the Hauptman-Woodward Institute in Buffalo to enable high throughput screening of 1536 possible conditions. Based on the preliminary crystal screens done at McMaster, a protein concentration of 4 mg/mL was selected for this high-throughput screen. Drops were set by the liquid handling robot in the micro-batch under oil method (29). Photos of each drop were taken immediately after the addition of protein, one day after initial set up, and subsequently once a week for four weeks. Images were viewed with the use of Macroscope software.

3.2.3. Modelling of EreB structure

Modelling of EreB was performed with the help of Dr. Maria Morar. The *E. coli* EreB sequence was input into the PSIPRED Protein Structure Prediction Server (30) to predict secondary structure, and EreB structural homologs were searched for with the use

of profile-profile prediction method pGENthreader. This method uses secondary structure predictions and alignment output from PSIPRED to search for proteins with similar folds. The sequence alignments generated by pGENthreader predicted that EreB would share the highest fold similarity with two structures: PDB ID 3b55 and 2qgm. The alignments with these two structures and their atom coordinates were used in making of the EreB structural homology model. Modeller 9v7, a program for comparative protein structure modelling by satisfaction of spatial restraints, was used for this purpose (19). The script file was generated by using model-default.py input file as a template with the default settings. Coot and PyMOL were used for the visualization and overlaying of the EreB homology model with the existing PDB structures 3b55 and 2qgm.

3.3 Results

3.3.1 Analytical Gel Filtration

By analytical gel filtration, the molecular weight of EreA was observed to be about 88 kDa. This was similar to that observed for EreB, with an apparent molecular weight of 83 kDa by analytical gel filtration, compared with a molecular weight of about 45 kDa for both enzymes by SDS-PAGE (see Table 3-1). A sample chromatogram from the gel filtration experiment with EreB is shown is Figure 3-1, and it can be seen that there is a single peak at an elution volume of 14 mL. By gel filtration, then, it appears both of these enzymes exist as dimers in their native state. In contrast, the oligomeric state of Ere-bc was found to likely be a monomer, based on its elution from a calibrated gel filtration column. This was consistent with the results of the NESG group that first purified Bcr136 (Ere-bc) for structural studies. Ere-se was also found to likely exist as a monomer, based on gel filtration, with the major peak observed being consistent with a

molecular weight of about 40 kDa. The inability of Ere-bc and Ere-se to hydrolyze erythromycin (as demonstrated in Chapter 2, section 2.3.5) may be due to these enzymes' inability to form dimers, which may constitute the active form of the protein.

Table 3-1. Predicted and observed molecular weights for the erythromycin esterases, and predicted oligomeric state

Esterase	Predicted molecular weight (kDa)	Molecular weight by SDS-PAGE (kDa)	Molecular weight by analytical gel filtration (kDa)	Oligomeric state
EreA	44.7	40	88	dimer
EreB	48 .2	42	83	dimer
Ere-se	42.2	40	39	monomer
Ere-bc	50.5	54	60	monomer

.

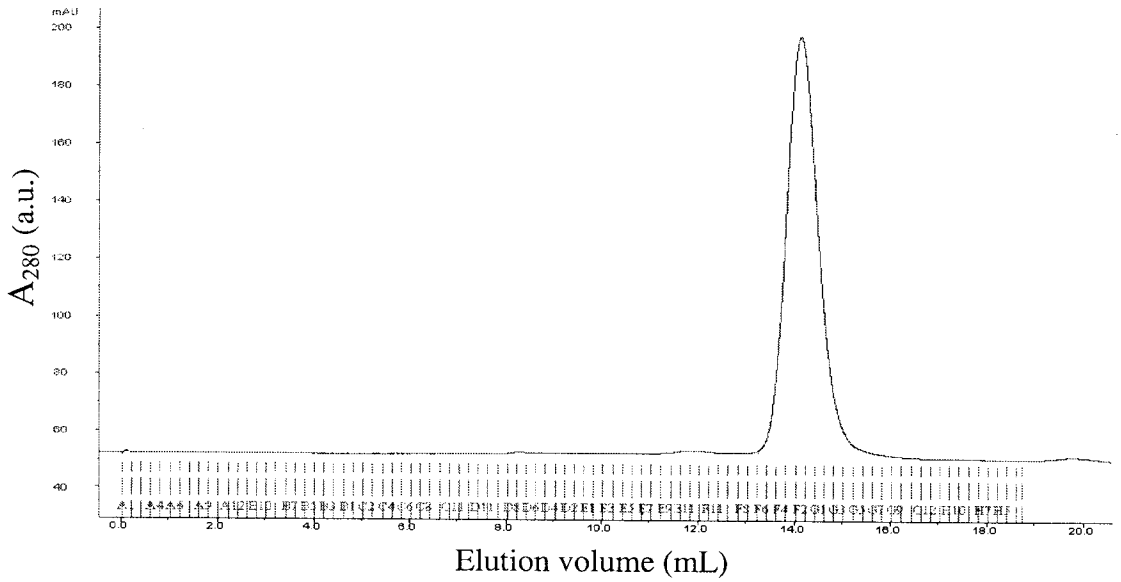

Figure 3-1. Sample chromatogram of EreB elution from a Superdex-200 10/300 GL column

Previously, an EreA-like protein was purified by Kim et al. from a *Pseudomonas* species found in a Washington fish hatchery (25). This protein was identified based on N-

terminal sequencing, and was thought to be similar to that found in *P. stuartii*. This EreA-like protein was found by analytical gel filtration to exist as a monomer (25). Interestingly, our use of analytical gel filtration here suggested that the *P. stuartii* EreA exists as a dimer, with an apparent molecular weight of 88 kDa. The ability of this EreA-like protein to hydrolyze erythromycin is not consistent with our proposal that dimer formation may be necessary for catalysis.

3.3.2. Crystallization trials

For EreB in-house initial screens, one potentially promising hit was found in the Classics screen containing 0.2 M magnesium formate and 5 mg/mL EreB, with the appearance of rod-like crystal clusters after one week's growth. Optimization of this initial hit was then attempted, by varying the EreB concentration, the concentration of magnesium formate, the pH of each drop, and the ammonium sulfate content of the reservoir. Although it was possible to reproduce the original hit with various concentrations of EreB and 0.2 M magnesium formate solution from the Classics screen, this hit could not be reproduced without using that same tube of magnesium formate solution. During optimization, it was observed that similar crystals to those in the initial hit would grow in the presence of magnesium formate solution from that same Classics tube even in the absence of protein, meaning the crystals initially observed were likely not protein, but rather salt.

High-throughput screens from the Hauptman-Woodward Institute gave rise to some promising leads in terms of crystallization conditions. Specifically, the condition of 0.1 M NH_4SCN, 0.1 M TAPS pH 9 and 40% PEG 1000 yielded small single crystals.

Optimization of this condition was attempted in-house, but so far, no protein crystals have been obtained.

For EreA, initial in-house screens yielded some small crystal clusters were observed in a condition containing 10% PEG 3000, 0.1 M imidazole pH 8.0 and 0.2 M Li_2SO_4, but these clusters did not stain blue with the addition of "Izit Crystal Dye" (Hampton Research), suggesting that these crystals were most likely salt. This dye can aid in the detection of true protein crystals, as the dye is able to penetrate the solvent channels found in biological macromolecular crystals but is not able to enter a more tightly packed salt crystal. Some tiny crystal clusters found in a condition with 10% 2-propanol, and MES pH 6.0, and 0.2 M $Ca(OAc)_2$ did stain blue with the addition of 0.5 µL of a 1/20 dilution of "Izit Crystal Dye". However, so far optimization of this condition has not yielded crystals large enough to test in an x-ray beam, the only certain method for determining if crystals are salt or protein.

In the absence of protein crystals suitable for diffraction experiments, an alternative approach of structure modelling was taken to gain some possible insights into the three–dimensional structures of this family of proteins.

3.3.3. Modelling of EreB

According to the results generated from the pGENthreader program, *E. coli* EreB is predicted to share the most structural similarity with PDB deposited protein structures 3b55 and 2qgm. Both proteins are annotated as succinoglycan biosynthesis proteins from *B. cereus*, and EreB shares 21% and 24% of sequence identity (40% and 43% similarity) with 3b55 and 2qgm respectively. Both structures are the result of efforts by Northeast Structural Genomics Consortium and neither has been reported in the literature. The

pGENthreader structural alignment of EreB with PDB deposited protein 2qgm, or Ere-bc is illustrated in Figure 3-2. Conserved regions in this alignment are consistent with those generated by ClustalW for other annotated EreB sequences.

```
                10        20        30        40        50        60
          CCCCHHHHHHHHHHHHCCCCCCCCCCCCCCHHHHHHHCCCCCCCEEEECCCCCCCCHHHHCC
2qgm      SGQSVQKNIVKSIQSQANPLKTIEPSKPFEDLKPLKKMIGNAQYVGLGENTHGSSEIFTM
EreB      ------MRFEEWVKDKHIPFKLNHPDDNYDDFKPLRKIIGDTRVVALGENSHFIKEFFLL
          ------CCHHHHHHHCCEECCCCCCCCCCHHHHHHHHHHCCCCEEEEECCCCCCHHHHHH
                      10        20        30        40        50

                70        80        90       100       110
          CHHHHHHHHHCCCCCEECCCCCHHHHHHHHHHHHHCCCCCC--CCCCCCCCCHHHHCCCC
2qgm      KFRLVKYLVTEMGFTNFAMEEDWGNGLKLNEYIQTGKGNPR--EFLKLLYPTDEIIAMIE
EreB      RHTLLRFFIEDLGFTTFAFEFGFAEGQIINNWIHGQGTDDEIGRFLKHFYYPEELKTTFL
          HHHHHHHHHHHCCCCEEEEECCCHHHHHHHHHHCCCCCHHHHHHCCCCCCCCCHHHHHHHH
              60        70        80        90       100       110

               130       140       150       160       170
          CCCHHHHCCCCCCCCEECCCCCCCCC---HHHHHHHHHHHHHHCCCCHHHHHHHHHCCCC
2qgm      WMKDYNADPSNKKKIQFIGLDLKALD---QGSFNKVIDYVRLHRPDLLAEVEENYKELSS
EreB      WLREYNKAA--KEKITFLGIDIPRNGGSYLPNMEIVHDFFRTADKEALHIIDDAFNIAKK
          HHHHHCCCC--CCCEEEEEECCCCCCCCHHHHHHHHHHHHHHHHCHHHHHHHHHHHHHCCC
             120       130       140       150       160       170

           180       190       200                   210
          CCCCCCCCC-----CCCHHHHHHHHHHHHHHHHHC------------CCCCHHHHHHHH
2qgm      FTGSIQEYM-----KLTPKLKEKFKANAERVARLL------------KDEEYIWAKATA
EreB      IDYFSTSQAALNLHELTDSEKCRLTSQLARVKVRLEAMAPIHIEKYGIDKYETILHYANG
          CCCCCHHHHHHHHHHHCHHHHHHHHHHHHHHHHHHHHHHHHHHHHCCCHHHHHHHHHHHH
               180       190       200       210       220       230

          220       230       240       250       260       270
          HHHHHHHC-----CCCCCCCHHHHHHHHHHHHHHCCCHHHHHC--CCCCCCCCHHHHCCC
2qgm      SAIEKFTT-----MLLPNDYPSIIKLHEQYLADHAMWAQETFG--GKTMVWAHNIHIAKG
EreB      MIYLDYNIQAMSGFISGGGMQGDMGAKDKYMADSVLWHLKNPQSEQKVIVVAHNAHIQKT
          HHHHHHHHHHHHHCCCCCCCCCCCCCCHHHHHHHHHHHHHHHHHHCCCCCEEEEECCCCCCCC
               240       250       260       270       280       290

               280       290       300       310       320
          CC--CCCCCCCCHHHHHHHHHHHHHEEEEEEEEEEEEEEEC-----CCCCCC--EEEECCC
2qgm      II--DEKLYPYVAGQFLKERLDNNYVTIGSTTTEGNFTLY-----SEYGKI--TTDTIPQ
EreB      PILYDGFLSCLPMGQRLKNAIGDDYMSLGITSYSGHTAALYPEVDTKYGFRVDNFQLQEP
          CCCCCCCCCCCCCHHHHHHHHHCCCEEEEEEECCCCEEECCCCCCCCCCCCCCCCEEEECCCC
               300       310       320       330       340       350
```

```
                330        340        350        360        370        380
          CCCCHHHHHHHCCCCCCEEECCCCCHHHHHHHHHCEEEEECCCCCCCEEEEEHHHHCCEEE
2qgm      DVKSFNYTLGKVPYKMFLLDNRHLKGQAEKWVKAKRPLLSIGGQIVYFDTSLLEQFDIIF
EreB      NEGSVEKAISGCGVTNSFVFFRNIPEDLQSIPNM------IRFDSIYMKAELEKAFDGIF
          CCCCHHHHHHHCCCCCEEEECCCCCHHHHHCCCC------CCCCCCCCCCCHHHHCEEEE
               360        370        380              390        400

                390
          EEEEECCCCCC--
2qgm      HIRKTSPSHIK--
EreB      QIEKSSVSEVVYE
          EECCCCCHHHCCC
           410
```

Figure 3-2. pGENthreader alignment of *E. coli* EreB predicted protein sequence with that of PDB 2qgm, NESG target protein Bcr136. C stands for coil, H – helix, E - sheet.

The homology model of the EreB structure produced by Modeller was found to be in good agreement with the primary structure alignments. The insertions found in the EreB sequence were located in loop regions and did not appear to disrupt the secondary structural elements and the conservation of the overall fold (Figure 3-3 A). The EreB homology model predicts that this protein has a structure consisting of two domains. The first domain contains an αβ-structure with a central mixed β-sheet of 7 strands, flanked by 5 α-helices, while the second domain contains a 4 α-helix bundle (Figure 3-3 B).

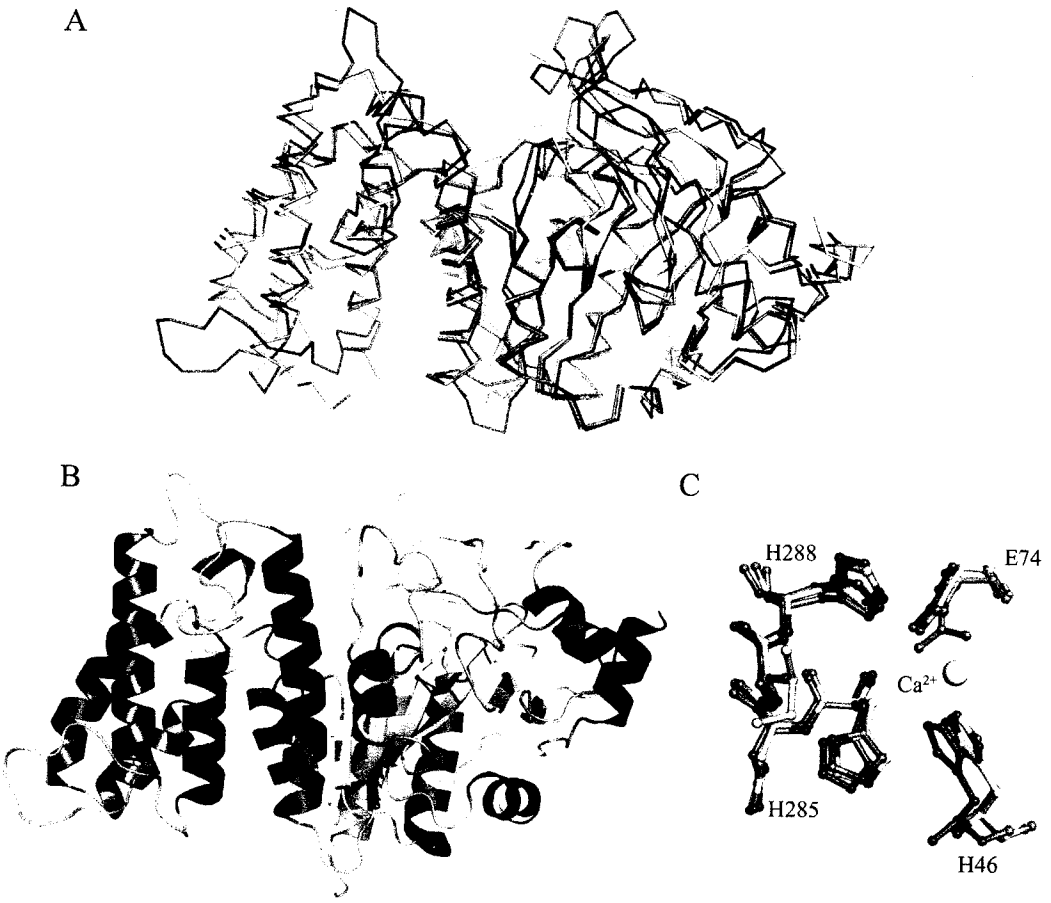

Figure 3-3. EreB homology model. (A) Superposition of EreB model (blue) with structures 2qgm (green) and 3b55 (grey). (B) Cartoon diagram of the EreB homology model high-lighting domain organization and secondary structure. (C) Superposition of the predicted catalytic residues of the EreB homology model putative active site (blue) with residues from 2qgm (green) and 3b55 (grey). Residue numbering is of *E. coli* EreB.

A putative active site pocket is located in the cleft formed by the two domains. In the 3b55 structure, the location of this pocket is marked by the presence of a Ca^{2+} ion. Conserved and potentially catalytic residues His285, His288, His46, and Glu74 (*E. coli* numbering) are all located in this putative active site (Figure 3-3 C). The clustering of conserved residues in this region lends support to the hypothesis that these residues may be important for catalysis. The amide moieties of residues 286, 287, and 288 from the strictly conserved HNXH sequence shape a loop positioned and oriented properly for the

formation of an oxyanion hole, which could potentially be necessary for the stabilization of a tetrahedral intermediate in catalysis. Selected residues in this region of EreB have therefore been targeted for site-directed mutagenesis, the results of which will be discussed further in Chapter 4.

3.4 Summary and Conclusions

In the absence of a crystal structure for EreA or EreB, it is still possible to make some inferences about protein structure. Gel filtration was used to determine the oligomeric state of these two proteins, and it was found that both EreA and EreB exist as dimers. In contrast, the putative erythromycin esterases from *B. cereus* and *S. erythraea* were found to exist as monomers.

The complete genome of *Bacillus cereus* ATCC 14579 has been sequenced (23).Within this genome, the two proteins Bcr136 and Bcr135 have been annotated as succinoglycan biosynthesis proteins, but share sequence identity to erythromycin esterase from *E. coli* at around 20-24% (40-43% similarity). Additionally, genomes from other *B. cereus* strains, and from species such as *Bacillus thuringiensis* contain genes annotated as putative erythromycin esterases that code for proteins with 95% identity to these "succinoglycan biosynthesis" proteins. Furthermore, no homology is seen between Bcr135 or Bcr136 and any of the enzymes in the known succinoglycan biosynthesis pathway (22). It is possible that the annotations in *B. cereus* ATCC 14579 are incorrect, and these proteins are, in actuality, esterases. Since structures have been determined for Bcr136 and Bcr135, these structures were used here to create a structural model for EreB. Conservation of primary amino acid sequence is not always a good indicator of whether or not two proteins will share a similar fold. For example, Bcr135 and Bcr136 share only

37 % identity (58% similarity) at the primary sequence level, but the overall folds of these two proteins are extremely similar.

In our studies, NESG target protein Bcr136, or Ere-bc was not found to exhibit activity against erythromycin or other macrolides. It was, however, shown to have esterase activity, as seen by its ability to hydrolyze the substrate *p*-nitrophenyl butyrate (see Chapter 2 section 2.3.2.2), among other *p*-nitrophenyl esterase substrates. Either this protein's natural activity is as an esterase for some unknown molecule, or this observed esterase activity is a secondary one, a by-product of its natural function as, say, a protease. It may be that this protein could act on erythromycin if some key mutations were made in the enzyme's active site.

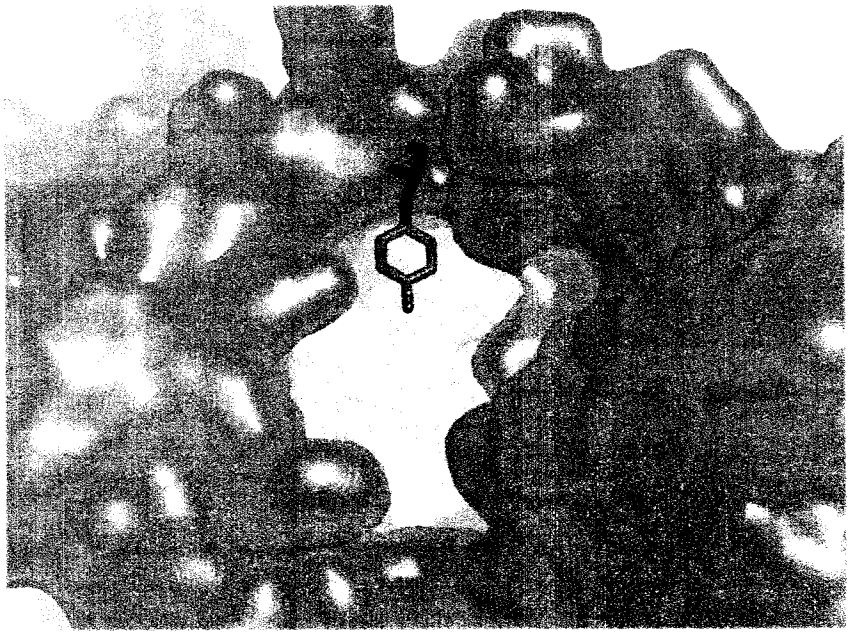

Figure 3-4. Surface view of EreB model with predicted active site cleft shown in red. Tyrosine residue 320 from Bcr136 is superimposed and shown in cyan.

For this reason, the putative active site of Bcr136, as observed in the PDB structure 2qgm was compared to that of EreB in the generated model. It was found that

few differences existed between the amino acids present in this region, as well as their orientation. One key difference was observed at position 320, where a serine residue is present in the EreB model, whereas in Bcr136, a tyrosine residue is in this position (see Figure 3-4). It was proposed that the bulky nature of the tyrosine residue may hinder the protein's ability to accept the large erythromycin molecule as a substrate. Therefore, the mutation of Y320S was investigated as a possible single mutation that could give rise to the ability of Bcr136 to act as an antibiotic resistance protein.

Chapter 4 – Investigation of Enzyme Mechanism for the Erythromycin Esterases

4.1 Overview

Since erythromycin esterases hydrolyze the ester bond of the lactone ring, it is possible that the enzymatic mechanism of these proteins follows that of other known hydrolytic enzymes, such as the proteases. For example, Ere proteins could act via a catalytic triad in a manner similar to the serine proteases, or use the SH group of a cysteine residue as a nucleophile like the cysteine proteases. Alternatively, they may rely on a chelated metal ion like zinc for catalysis as with the metalloproteases (46). Some of these mechanistic possibilities have been examined through a number of methods, including the use of inhibitors, examination of alignments for identification of conserved residues, site directed mutagenesis, and by studying the effect of pH on kinetic parameters. Some differences between EreA and EreB were found and are of particular interest.

4.2 Methods

4.2.1. Amino acid sequence alignments

Predicted protein sequences for erythromycin esterases from a number of source organisms were obtained from NCBI, selected based on protein sequence similarity with EreB in a BLAST search. Alignments were performed using both ClustalW, and with the help of Dr. Brian Golding, MUSCLE (17) . Boxshade was used to aid in the visualization of conserved residues.

4.2.2. Inhibition studies

The possibility of ethylenediaminetetraacetic acid (EDTA) and phenylmethylsulfonyl fluoride (PMSF) to inhibit the activity of the Ere proteins was

investigated using the *p*-nitrophenyl butyrate continuous assay as described in Chapter 2. Reactions contained 1 mM or 10 mM of either EDTA or PMSF, and were initiated by the addition of enzyme pre-incubated with 1 or 10 mM inhibitor for 10 minutes.

4.2.3. Site-directed mutagenesis and characterization of mutant proteins

Sites for mutagenesis were selected based on conserved amino acid residues identified with alignments of erythromycin esterases, and the putative active site within the EreB structural model. Mutations were generated with the use of the QuikChange Mutagenesis Kit (Stratagene) and the following oligonucleotide primer pairs (see Table 4-1). Mutations were verified by DNA sequencing (MOBIX, McMaster University) with the use of plasmid specific primers.

Minimum inhibitory concentrations (MIC) for erythromycin were determined for *E. coli* BL21 (DE3) cells expressing these mutant proteins, as described in Chapter 2. Activity of purified mutant proteins as esterases was examined using the *p*-nitrophenyl butyrate continuous assay as performed for wild-type protein. The ability of these mutants to inactivate erythromycin specifically was probed by incubation of enzyme with drug and testing for remaining biological activity of the macrolide against *Micrococcus luteus*.

Table 4-1. Primer pairs used in the generation of site-specific mutations for EreA, EreB, and Ere-bc. Codons targeted for mutagenesis are shown in bold.

Esterase	Mutation	Primer Pair (5' → 3')
EreA	E68A	Forward CGATTGGTTTG**GCG**TGTGGGGCG Reverse Complement CGCCCCACA**CGC**CAAACCAATCG
EreB	E74A	Forward CGTTTGCTTTT**GCA**TTTGGTTTTGCTG Reverse Complement CAGCAAAACCAAA**TGC**AAAAGCAAACG
	H288A	Forward GTGATAGTAGTAGCACATAATGCA**GCT**ATTCAAAAA ACACCC Reverse Complement CCATCATACAGAATGGGTGTTTTTTGAAT**AGC**TGCAT TATGTGCTACTACTATCAC
Ere-bc	Y320S	Forward AGCTAAAGGAATTATCGATGAGAAATTA**AGC**CCTTA TGTTGCGGGGC Reverse Complement GCCCCGCAACATAAGG**GCT**TAATTTCTCATCGATAAT TCCTTTAGCT
Ere-sc	N241H	Forward CCTGCTCGCCTCC**CAC**AATGGCCACGT Reverse Complement ACGTGGCCATT**GTG**GGAGGCGAGCAGG

4.2.4. pH studies

The dependence of kinetic parameters on pH was determined for EreA and EreB with the use of the continuous spectrophotometric assay and *p*-nitrophenyl butyrate as the

substrate. The various buffer systems used were as follows, each at 50 mM: pH 6.0-6.5 MES, pH 6.5 – 7.5 MOPS, pH 7.0 – 8.0 HEPES, pH 8.0 – 9.0 TAPS. Standard curves were prepared for the absorbance of known concentrations of the coloured product *p*-nitrophenol at 405 nm under each buffer condition, in order to allow for conversion of absorbance to product concentration. Data were analyzed by nonlinear least-squares method, and fit to Equation 1 with Grafit 4.0.21 (Erithacus software). Kinetic parameters were then fit to Equation 2 or 3 using Gnuplot (version 4.2.5), where Y refers to the varied parameter (V_{max} in Equation 2, V_{max}/K_m for Equation 3), C refers to the limiting value of this parameter, [H^+] refers to the concentration of hydrogen ions, and K_1 and K_2 are the ionization constants.

$$v = (k_{cat}/E_t)[S]/(K_m + [S]) \qquad [1]$$

$$Y = C/(1 + [H+]/K_1) \qquad [2]$$

$$Y = C/(1 + [H+]/K_1 + K_2/[H+]) \qquad [3]$$

4.2.5. Solvent Isotope Effects on EreA and EreB

The solvent isotope effect on the hydrolysis reactions carried out by erythromycin esterases EreA and EreB was examined using the *p*-nitrophenyl butyrate continuous assay in the presence of both water and D_2O. In this experiment, 250 µL reactions containing 50 mM HEPES pH 7.5, between 15.6 µM and 2000 µM p-NPB substrate, and 0.1% Triton-X100 were initiated with the addition of 0.02 mg enzyme. In these reactions, D_20 accounted for 84% of the solvent present. Standard curves with the reaction product *p*-nitrophenol, were prepared fresh in reaction buffer containing D_2O in order to correct for any change in absorbance at 405 nm that may occur due to the change in solvent. Reactions were allowed to proceed for 45 minutes, during which the absorbance at 405

nm was recorded once every minutes. Data were analyzed using nonlinear least-squares method and Grafit 4.0.21 (Erithacus software), and fit to Equation 1 above. Kinetic parameters were then compared with those obtained for each enzyme in buffer containing H_20. Since pH is not equal to pD, but rather pD = pH + 0.5 (45), kinetic parameters for EreA and EreB in HEPES pH 8.0 were used for comparison.

4.3. Results

4.3.1. Alignments

Although the sequence similarity of erythromycin esterases at the protein level is relatively low (around 30% identity), the examination of amino acid alignments did reveal some conserved regions that may suggest important residues for protein function.

In terms of potential enzyme mechanisms, the amino acid sequences in Figure 4-1 were examined for common motifs shared by other hydrolytic enzymes, like serine proteases. A classic catalytic triad of serine, histidine and aspartate residues was not seen, since there are no universally conserved serine residues within the aligned sequences. Additionally, it is unlikely that the Ere proteins rely on a cysteine residue for catalysis since there are no conserved cysteines observed in the aligned sequences. A conserved motif does emerge when examining these proteins consisting of a histidine residue, followed by asparagine, another amino acid the identity of which is not conserved between species, and finally another histidine, (HNXH), shown in Figure 4-1 in red. In the structure determined for Ere-bc, and in the generated EreB model, this motif maps to the cleft between the two domains of the protein, an area which may be the active site. The conserved glutamate found at position 74 (*E. coli* numbering) also maps to this region in the structural model. The importance of some of these conserved residues for

protein activity has been further investigated here, through the use of site-directed mutagenesis.

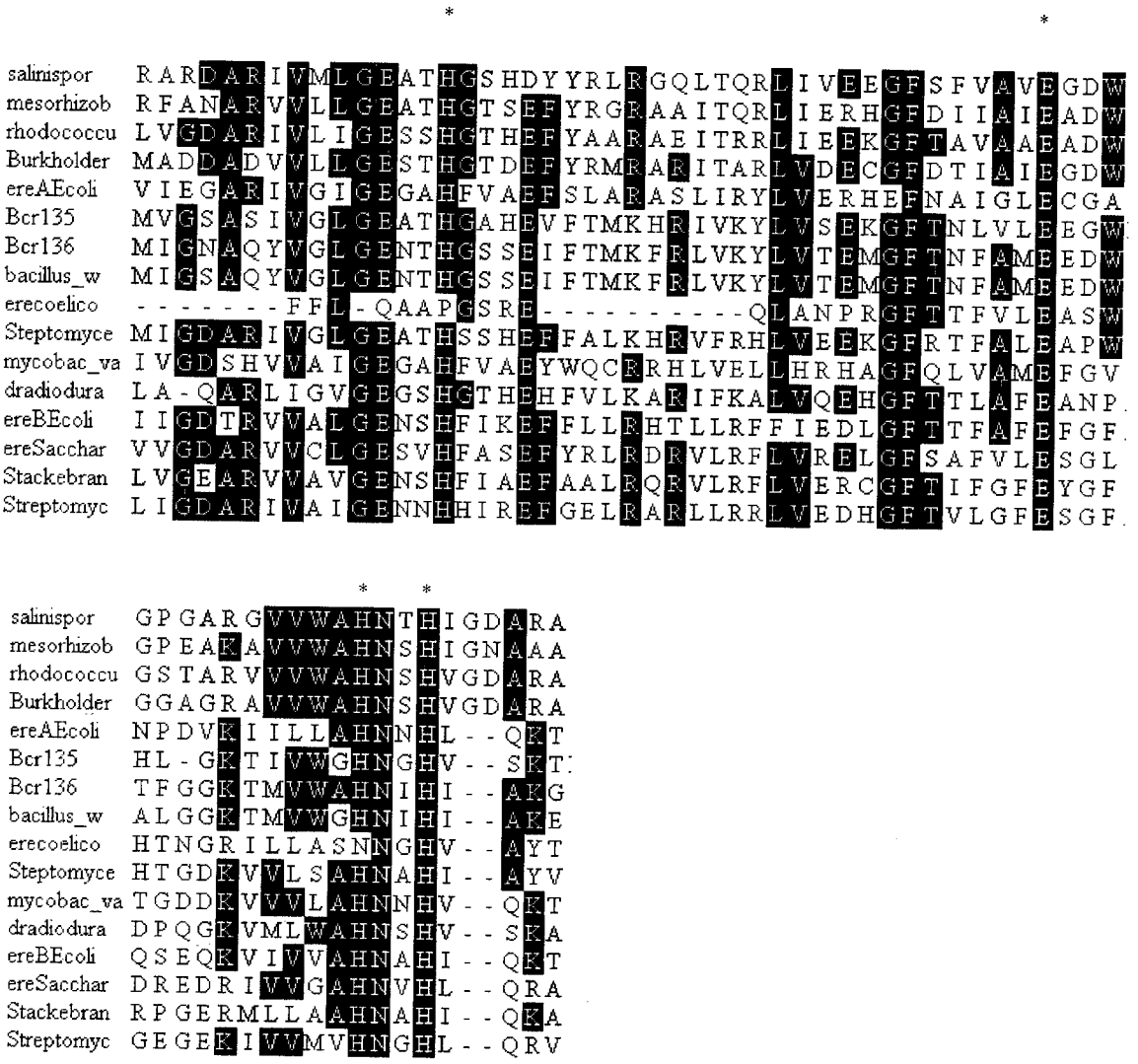

Figure 4-1. Selected regions from MUSCLE alignment of protein sequences for select erythromycin esterases (both known and putative) from a variety of organisms. Identical residues are shown in black, while similar residues are highlighted in grey. Residues conserved in all sequences are highlighted in red, and * marks conserved residues located in the putative active site. Shading was done using the Boxshade program v.3.2.1.

4.3.2. Inhibition studies

Phenylmethylsulfonyl fluoride (PMSF), which binds irreversibly to serine residues and inhibits catalysis of serine proteases, was not found to be an inhibitor of the inactivation of erythromycin by either EreA or EreB. EDTA, a metal chelator that may inhibit enzymes relying on the presence of a metal ion for catalysis, was also not found to inhibit either of these enzymes when erythromycin was used as a substrate. With *p*-nitrophenyl butyrate as the substrate, again, both PMSF and EDTA were not found to be inhibitors of EreA or EreB activity, and additionally did not have any effect on the esterases Ere-se or Ere-bc. A sample progress curve for the reaction of EreA with *p*-NPB in the presence and absence of 1 mM EDTA and PMSF is shown below.

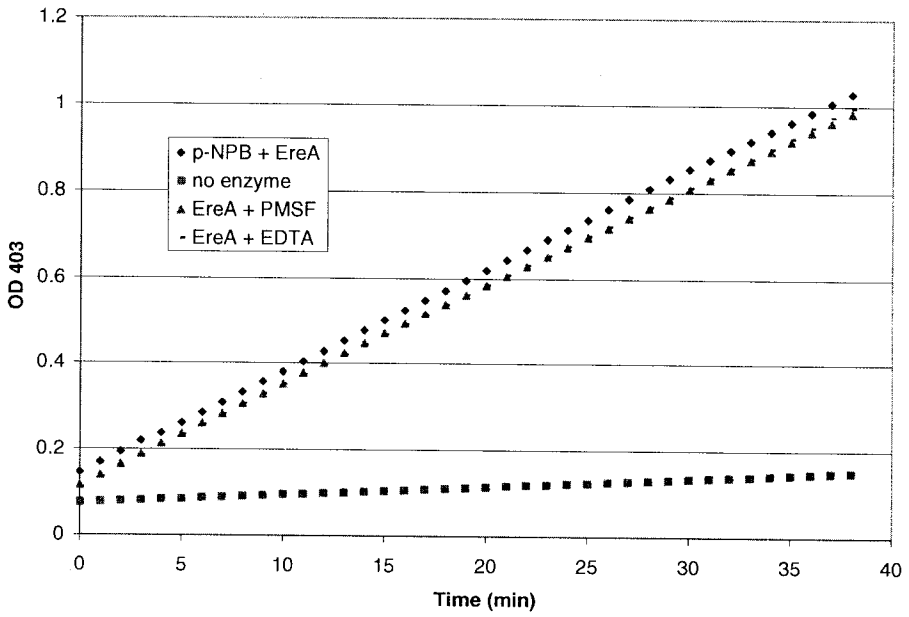

Figure 4-2. Sample progress curve for the release of *p*-nitrophenol over time in 250 µL reactions of 0.02 mg EreB (or no enzyme control) with 2.3 mM *p*-nitrophenyl butyrate, in presence or absence of 1mM PMSF or EDTA. Reactions were initiated by addition of enzyme pre-incubated with 1mM PMSF or EDTA for 10 minutes.

4.3.3. Site-directed Mutagenesis and Characterization of Mutant Proteins

4.3.3.1. MIC determinations for selected site mutants

The minimum inhibitory concentrations of erythromycin against *E. coli* BL21 (DE3) cells harbouring *ere* genes with selected mutations were established. The expression of wild-type EreA or EreB lead to a marked increase in MIC values, from 64 μg/mL in cells not expressing an Ere protein, to 1024 μg/mL and >2048 μg/mL for EreA and EreB respectively. The mutation of glutamate to alanine at position 74 (E74A) in EreB was found to reduce the MIC of *E. coli* to 64 μg/mL, the same value as in cells harbouring an empty plasmid. Likewise, the histidine to alanine mutation at position 288 (H288A) was found to reduce the MIC value to background level, 64 μg/mL. These changes in MIC value may indicate a loss in function for these proteins due to disruption of the active site, but may also reflect loss of function due to structural problems with protein folding, or be due to lowered expression levels or reduced solubility with these mutants.

Table 4-2. MIC's of erythromycin against *E. coli* BL21 (DE3) harbouring *ere*'s from different source organisms, with selected site mutations present

Ere and plasmid vector	Mutations present	MIC μg/ml
pDEST14-EreA	wt	1024
	E68A	128
pDEST14-EreB	wt	>2048
	E74A	64
	H288A	64
pDEST14-Ere-se	wt	64
pET22b-Ere-sc	wt	64
	N241H	64
pET21b(+)-Ere-bc	wt	64
	Y320S	256
pET28a(+)	-	64

Alternatively, the tyrosine to serine mutation at position 320 in the *B. cereus* putative Ere was found to increase the MIC value four-fold from 64 μg/mL when wild-type protein is expressed, to 256 μg/mL. Although the wild-type protein does exhibit esterase activity when evaluated in the *p*-nitrophenyl butyrate assay, the wild-type Ere-bc was not found to have activity against erythromycin or other macrolide antibiotics. No increase in MIC was observed for the N241H mutation in the *S. coelicolor* putative Ere. This mutation restores the HNXH motif that is incomplete in the Ere-sc protein, but the lack of change in MIC value suggests this mutation alone cannot alone introduce erythromycin esterase activity. However, since this protein was not able to be purified, the lack of resistance phenotype observed for both the wild type and the N241H mutant strains may be due to poor protein expression or problems with proper folding in the *E. coli* expression host. For all other mutations, in order to test whether changed MIC values did correspond to loss or gain of erythromycin esterase function, mutant proteins were purified and their activity quantified with respect to wild-type.

4.3.3.2. Activity of purified site mutants

The activity of purified enzymes containing the mutations E74A and H288A (for EreB) and Y320S (for Ere-bc) was determined both by disc diffusion assay and spectrophotometric assay with *p*-nitrophenyl butyrate. The ability of these mutant proteins to inactivate erythromycin after one hour of incubation with antibiotic is shown below in Table 4-3. Although the E74A mutation was found to reduce the MIC value of erythromycin against *E. coli* cells expressing this protein to that of cells expressing only an empty expression vector, when purified, this protein was found to retain its ability to inactivate erythromycin. The H288A mutation however, was found to completely abolish

the ability of EreB to inactivate erythromycin. Even after incubation of erythromycin with 0.2 mg H288A EreB for 24 hours, no inactivation was seen. LC/MS was additionally used to verify the absence of any inactivation product.

Table 4-3. Activity of Ere enzymes against erythromycin, + indicates ability to completely inactivate a 50 μL reaction of 100 μM drug after 1 hr of incubation with 0.08 mg purified protein, as determined by Kirby-Bauer disc diffusion assay

Ere	Mutations	Activity against erythromycin	Activity against *p*-nitrophenyl butyrate	
EreB	WT	+	K_m	0.281 ± 0.012 mM
			k_{cat}	17.1 ± 0.22 s^{-1}
			k_{cat}/K_m	6.09 x 10^4 $s^{-1}M^{-1}$
	E74A	+	K_m	0.476 ± 0.053 mM
			k_{cat}	5.06 ± 0.24 s^{-1}
			k_{cat}/K_m	1.06 x 10^4 $s^{-1}M^{-1}$
	H288A	-	K_m	1.08 ± 0.21 mM
			k_{cat}	14.2 ± 1.3 s^{-1}
			k_{cat}/K_m	1.32 x 10^4 $s^{-1}M^{-1}$
Ere-bc	WT	-	K_m	0.896 ± 0.11 mM
			k_{cat}	34.1 ± 1.9 s^{-1}
			k_{cat}/K_m	3.81 x 10^4 $s^{-1}M^{-1}$
	Y320S	-	K_m	0.950 ± 0.084 mM
			k_{cat}	37.6 ± 1.5 s^{-1}
			k_{cat}/K_m	3.96 x 10^4 $s^{-1}M^{-1}$

Despite its inability to act on erythromycin, the H288A EreB mutant did retain some general esterase activity, as demonstrated by its ability to hydrolyze the esterase substrate *p*-nitrophenyl butyrate. As seen in Table 4-3, the k_{cat} for H288A against *p*-nitrophenyl butyrate was found to be 14.2 ± 1.3 s^{-1}, lower than that established for wild-

type EreB, 17.1 ± 0.22 s^{-1}. The *Km* value for the H288A mutant was found to be higher that that of the wild-type protein, resulting in the overall catalytic efficiency of the mutant protein being about five times lower than for wild-type, with a k_{cat}/K_m of 1.32 x 10^4 $s^{-1}M^{-1}$ compared to 6.09 x 10^4 $s^{-1}M^{-1}$.

For the putative erythromycin esterase from *B. cereus*, it was found that the Y320S mutant did not introduce new erythromycin esterase activity even after 24 hours incubation, despite the slightly higher MIC value for erythromycin against cells expressing this protein. The activity for *p*-nitrophenyl butyrate hydrolysis by this mutant was determined and was seen to have a k_{cat} value of 37.6 s^{-1}, comparable to that seen for the wild-type protein.

4.3.4. pH studies

The dependence of pH on the kinetic parameters of EreA and EreB was examined in order to shed some light on the enzyme mechanisms employed by these two proteins. From examining the pH dependence of the kinetic parameters V_{max} and V_{max}/K_m, it may be possible to identify particular residues important for catalysis, based on their ionization constants (18). When varying substrate concentrations for EreA, it was found that the maximum velocity of reaction varied with respect to pH, increasing to a maximum value around pH 8.0 (see Figure 4-3 A). Fitting of this curve to Equation 2 above, indicates there is a single pKa value of about 6.2, suggesting that the enzyme is most active when an ionizable group with a pKa of 6.2 is deprotonated. This may correspond to a histidine residue, since the pKa of histidine is around 6.0 (34). This was particularly interesting given the strict conservation of three histidine residues that map to the putative active site of both Ere-bc, and in the EreB model.

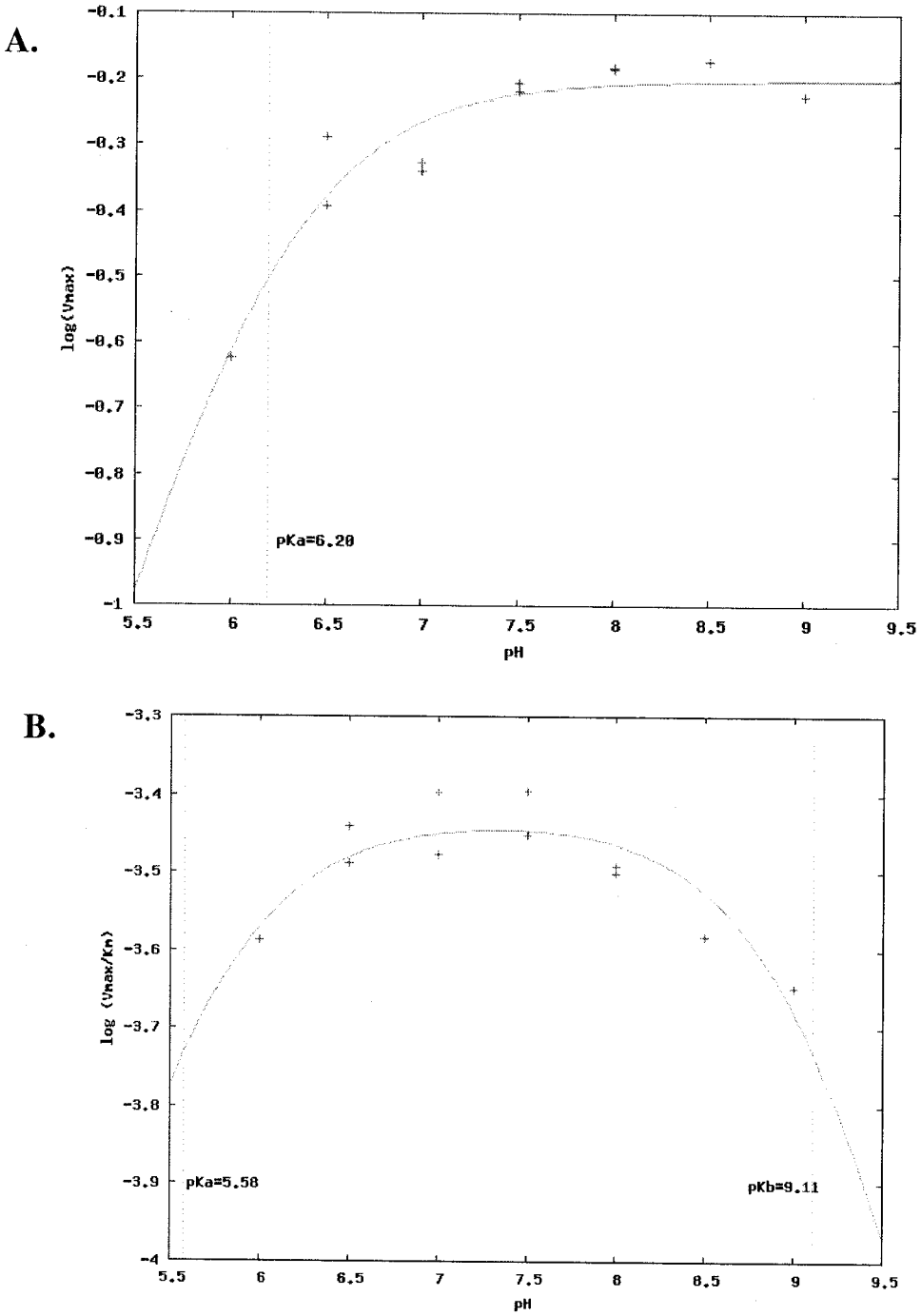

Figure 4-3 A. Dependence of log (V_{max}) on pH for EreA, pKa value of 6.20 shown at dotted line **B**. Dependence of log (V_{max}/K_m) on pH, pKa and pKb shown here at dotted lines to be 5.58 and 9.11 respectively.

For the dependence of V_{max}/K_m on pH, a different trend was observed, and the bell shaped curve generated yielded two ionization constants, a pKa of 5.58 and a pKb of 9.1.

This means that the enzyme is maximally active when one residue with pKa of 5.58 is deprotonated, and another group having a pKa of 9.1 is protonated. Again, the pKa of 5.58 could indicate the importance of a deprotonated histidine residue for catalysis. This also suggests the additional role of a residue with a pKa of 9.1.

Dependence of kinetic parameters on pH was repeated for EreB, with differing results. In this case, the dependence of V_{max} on pH did not yield a curve that could be fit to either Equation 2 or 3. It is possible that practical constraints that led to a lower limit of the assay of pH 6.0 (below which the yellow product *p*-nitrophenol cannot be reliably detected) resulted in not enough values being generated for the full picture of pH dependence on this enzyme's kinetic properties to be observed. Alternatively, this may reflect some differences between the residues necessary for catalysis in EreA and EreB.

4.3.5. Solvent Isotope Effect

The effect of solvent isotope on the reactions of EreA and EreB with *p*-nitrophenyl butyrate as a substrate were compared. For EreA, in a reaction containing H_2O as the primary solvent, it was found that the k_{cat} value was only 1.43 times larger than the value when the reaction was carried out in D_2O. With EreB, a slightly larger difference was seen, but the ratio of k_{cat} values in H_2O compared to D_2O was 2.15.

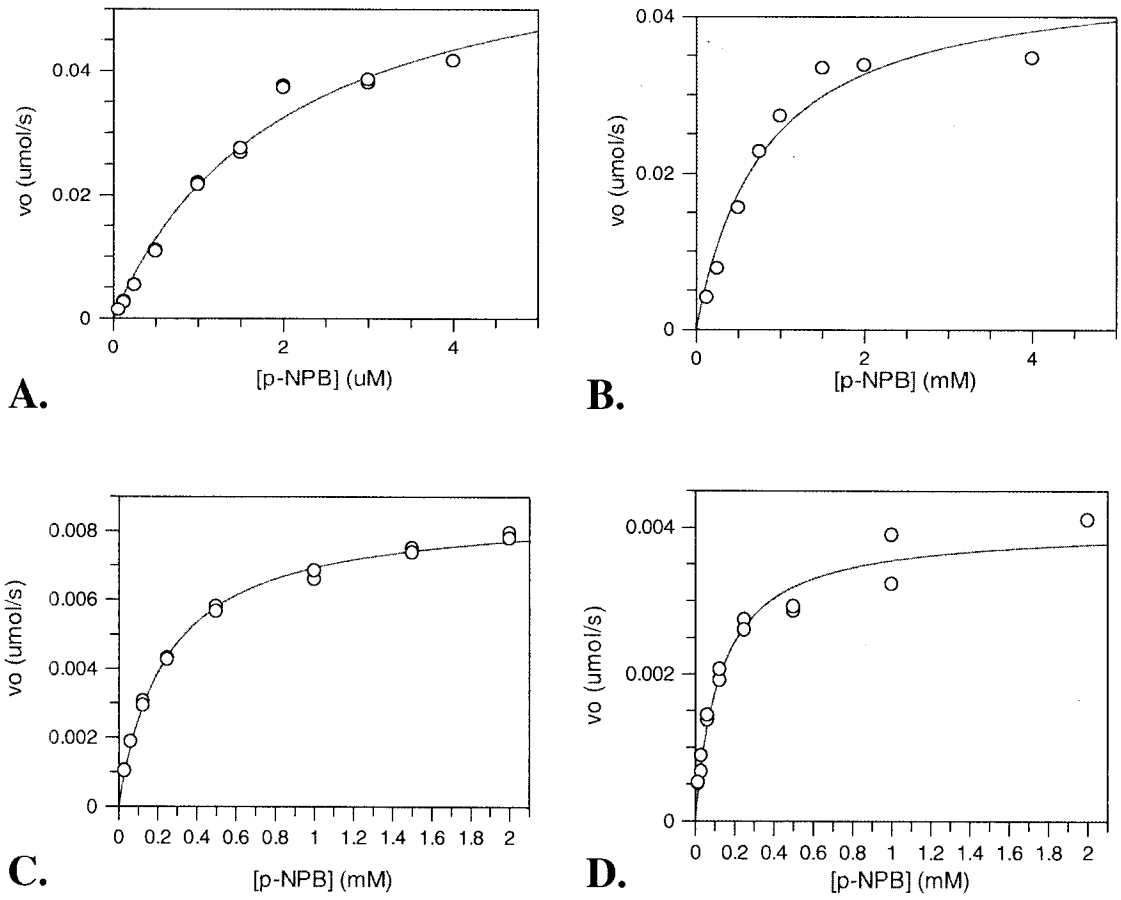

Figure 4-4. Michaelis-Menten curves for the determination of solvent isotope effect on kinetic parameters A. EreA in H_2O, B. EreA in D_2O, C. EreB in H_2O, D. EreB in D_2O

Table 4-4 Summary of kinetic parameters for solvent isotope effects on EreA and EreB

Esterase	H2O	D2O	SIE
EreA	K_m 2.03 ± 0.31 mM k_{cat} 146.5 x ± 11 s^{-1} k_{cat}/K_m 7.23 x 10^4 $s^{-1}M^{-1}$	K_m 0.807 ± 0.21 mM k_{cat} 102.6 ± 9.9 s^{-1} k_{cat}/K_m 1.27 x 10^5 $s^{-1}M^{-1}$	1.43
EreB	K_m 0.245 ± 0.01 mM k_{cat} 20.71 ± 0.33 s^{-1} k_{cat}/K_m 8.45 x 10^4 $s^{-1}M^{-1}$	K_m 0.128 ± 0.016 mM k_{cat} 9.65 ± 0.36 s^{-1} k_{cat}/K_m 7.53 x 10^4 $s^{-1}M^{-1}$	2.15

4.4 Summary and Conclusions

Based on the alignment of Ere protein sequences, and on some of the information generated., it is possible to evaluate some of the potential enzyme mechanisms employed by the erythromycin esterases. The absence of a conserved catalytic triad, and the ability to remain active in the presence of PMSF suggests EreA and EreB are not members of the serine protease family. In terms of metalloproteases, EDTA was not found to have any effect on the activity of either EreA or EreB suggesting that a chelated metal ion is not necessary for catalysis. These findings are consistent with those reported by Kim *et al.* (25) in which an EreA purified from an environmental *Pseudomonas* strain was also not inhibited by EDTA or PMSF. It is also unlikely that the Ere proteins rely on a cysteine residue for catalysis since there are no conserved cysteines observed in the aligned sequences.

The loss of activity observed when the histidine residue at position 288 (*E. coli* EreB numbering) is changed to an alanine residue, indicates this residue may be important for catalysis. Although this mutant's ability to hydrolyze erythromycin was completely abolished, it did still retain residual esterase activity as noted by its continued ability to hydrolyze *p*-nitrophenyl butyrate. However, values of k_{cat}/K_m were decreased about 5-fold for this mutation with respect to wild-type protein. It was found that the E74A mutation did not abolish the ability of EreB to hydrolyze erythromycin, although it did lower the values of k_{cat} and k_{cat}/K_m in the reaction with *p*-nitrophenyl butyrate, indicating that the catalytic efficiency of this protein was also decreased with respect to wild-type. His 288, then, is essential for activity, while E74 is not.

An examination of effects of pH on kinetic parameters for EreA suggested that a residue of pKa ~6.2 is important for catalysis. This likely corresponds to a histidine residue within the active site, consistent with the importance of H288A, and the presence of three conserved histidines within the putative active site in Ere-bc and the EreB model. Dependence of V_{max}/K_m also yielded a pK that suggests involvement of a histidine residue deprotonated for activity, with a pK of 5.58, as well as an additional residue having a pK of about 9.1. This may correspond to another important residue within the active site, for example, a lysine (with a predicted pK range of 9.4-10.6 (18).), or this higher pK value may indicate an ionization state of the substrate. As with any pH studies, results must be interpreted with caution, since the microenvironment of the active site can greatly affect the pK of residues within this environment.

Solvent isotope effects on the two proteins, although modest, did show a decrease in k_{cat} values when comparing reactions of these esterases with *p*-nitrophenyl butyrate in H_2O with those in D_2O. However, since these effects were only 1.43 and 2.15 for EreA and EreB respectively, it is difficult to make any assumptions about the dependence of a rate limiting step on proton abstraction from these experiments. Although an effect of between 2-4 is consistent for a hydrolysis mechanism in which general-base catalysis results in removal of a proton from a water molecule, and subsequent attack of water on the substrate (45), this is by no means conclusive.

Mutagenesis work, pH studies and the strict conservation of three histidine residues between Ere proteins in different species suggest histidine residue(s) play an essential role in catalysis. Further mutagenesis of H46 and H285, and the creation of double and triple histidine mutants may elucidate the exact residues necessary for

turnover. The Y320S mutation was not found to introduce erythromycin activity in Ere-bc, indicating that the tyrosine residue that appears to block the proposed active site cleft is not the only barrier to this enzyme's use of erythromycin as a substrate.

Chapter 5 – Summary and Future Work

5.1 Summary of work and proposal of potential catalytic mechanisms

The objective of this work was to express, purify and characterize some erythromycin esterases from differing source organisms, in order to better understand this mode of resistance to macrolide antibiotics. Previously identified erythromycin esterases from *E. coli* and *P. stuartii*, as well as the putative Ere's from *S. erythraea* and *B. cereus* were successfully purified. The hypothetical protein from *S. coelicolor* was not obtained, as to date, attempts at obtaining soluble protein have been unsuccessful. This work represents the first time any EreB has been purified and characterized, as well as the first purification and investigation of the putative esterase from *S. erythraea.* It also represents the first functional studies of Bcr136, annotated as a "succinoglycan biosynthesis" protein, but which here has been shown to posses esterase activity. Two enzyme assays have been developed, a stopped assay using [^{14}C]erythromycin and thin-layer chromatography, and a continuous assay for the monitoring of general esterase activity. A structural model for EreB has been developed based on the existing crystal structure of two proteins from *B. cereus,* and potentially catalytic residues have been explored with the use of site-directed mutagenesis. Finally, potential mechanisms utilized by this family of proteins have been explored, and two potential mechanisms are proposed here.

When expressed, both EreA and EreB were found to confer erythromycin resistance to otherwise susceptible cells. This was demonstrated by an increase in MIC values from 64 μg/ml to >1 mg/ml upon introduction of a plasmid carrying either *ereA* or *ereB.* When purified, both proteins were found to completely inactivate 100 μM erythromycin, clarithromycin or roxithromycin after one hour of incubation, as

determined by disc diffusion assay. Neither enzyme was found to be able to inactivate the ketolide telithromycin. These proteins showed a slightly different substrate specificity in that only EreB was capable of inactivating azithromycin, a 15-membered semi-synthetic derivative of erythromycin. LC/MS analysis of reaction products confirmed hydrolysis to be the mode of inactivation, as expected.

In contrast, expression plasmids including genes for putative erythromycin esterases from *S. erythraea*, *B. cereus*, and *S. coelicolor* were not found to introduce any erythromycin resistance to otherwise susceptible cells. After purification, the two putative esterases from *S. erythraea* and *B. cereus* were not found to exhibit any activity against erythromycin and other macrolides, consistent with the MIC values obtained. It is possible then, that these proteins may serve an alternate function within their cellular environments.

Based on the continuous assay using *p*-nitrophenyl butyrate as a substrate, both EreA and EreB were found to have very similar kinetic constants. Catalytic efficiency values for these two enzymes were found to be $9.03 \times 10^4\ s^{-1}M^{-1}$ and $6.09 \times 10^4\ s^{-1}M^{-1}$ respectively. When using the stopped [^{14}C]erythromycin TLC assay to look at kinetic values for EreB using its natural substrate, erythromycin, values for catalytic efficiency were higher, at $5.93 \times 10^7\ s^{-1}M^{-1}$. The higher catalytic efficiency when erythromycin is used as a substrate is consistent with the enzyme's preference for erythromycin over *p*-NPB.

Surprisingly, although the putative esterases Ere-se and Ere-bc were not able to hydrolyze erythromycin, they were able to act on other esterase substrates, including *p*-nitrophenyl butyrate. When utilizing this esterase substrate, catalytic efficiency values for

Ere-se were on the order of 10^2, two orders of magnitude less than those seen for EreA and EreB, while catalytic efficiency values for Ere-bc were more similar to those of EreA and EreB. These enzymes then, can act as esterases, and may truly be esterases with an alternative substrate within the cell, or perhaps have this activity as a by-product of another function. The genes encoding for these proteins may represent the area of the resistome known as precursor or proto-resistance genes, genetic elements that possess the potential for conferring antibiotic resistance if the selection pressure is there (51).

Based on the characterization performed in this work, two potential mechanisms by which EreA and EreB may catalyze the hydrolysis of erythromycin can be proposed. Based on the structural model of EreB, and mutagenesis of key conserved residues, the putative active site of this protein family was found to contain three potentially catalytic histidines, one of which, H288 (*E. coli* numbering) has been shown to be essential for activity with erythromycin as the substrate. The potential active site also includes a glutamate residue, E74, shown by mutagenesis to be non-essential for activity with erythromycin, but when replaced by an alanine, does reduce catalytic efficiency in the *p*-NPB assay.

The first proposed mechanism, shown below in Figure 5-1 involves the activation of water through a deprotonated histidine, and subsequent nucleophilic attack on the carbonyl carbon of the ester. A tetrahedral intermediate is then stabilized by the presence of an oxyanion hole, formed by backbone chain residues 286, 287, and 288.

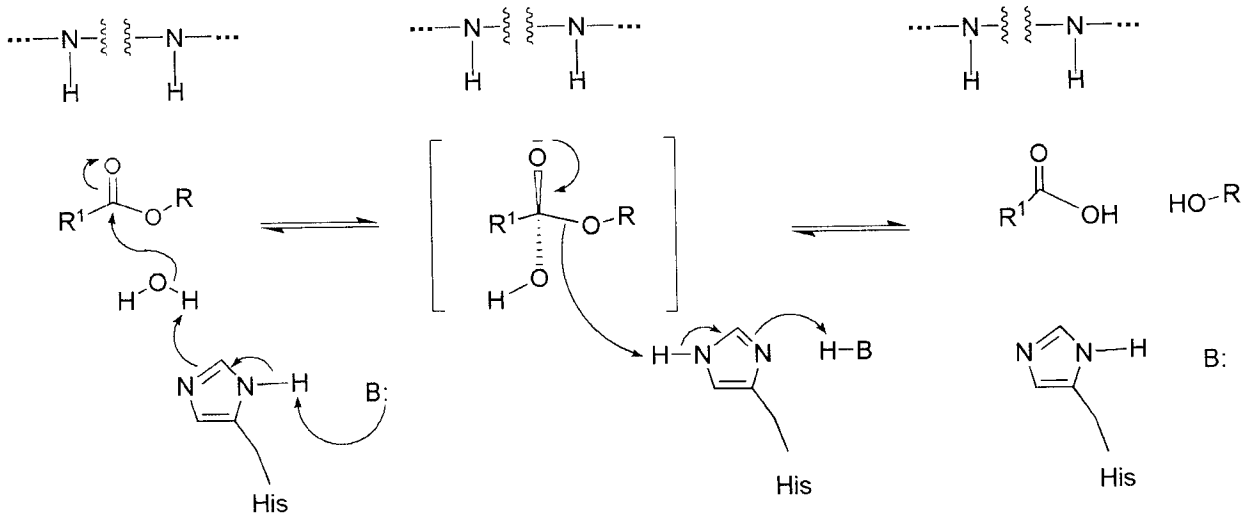

Figure 5-1. Mechanism 1 - Proposed mechanism of reaction for erythromycin esterase family involving activation of water and subsequent nucleophilic attack

This mechanism is consistent with the proposed active site by structural modelling of EreB, and mutagenesis studies, but seems inconsistent with solvent isotope effects seen for both EreA and EreB. If abstraction of a proton from water is the rate-limiting step for this reaction, one would expect to see a greater solvent isotope effect when using D_2O as the reaction solvent. The solvent isotope effects observed were 1.43 and 2.15 for EreA and EreB respectively. Solvent isotope effect, though, measures a more complex interplay of effects on rate (45), and it is possible that either substrate binding or product release could be rate limiting, thus masking any solvent isotope effect seen in D_2O for these enzymes.

Alternatively, another mechanism, involving the formation of an acyl-enzyme intermediate could be utilized by this family of proteins. This mechanism is shown below in Figure 5-2. Here a deprotonated histidine itself is responsible for nucleophilic attack, and again, a tetrahedral intermediate is stabilized by the formation of an oxyanion hole. Release of the alcohol results in the formation of an acyl-enzyme intermediate, which could, in theory, be isolated and detected. Finally, water, activated by perhaps another

histidine residue (there are three to choose from), performs a nucleophilic attack and hydrolysis of the acyl-enzyme intermediate occurs. Product is then released.

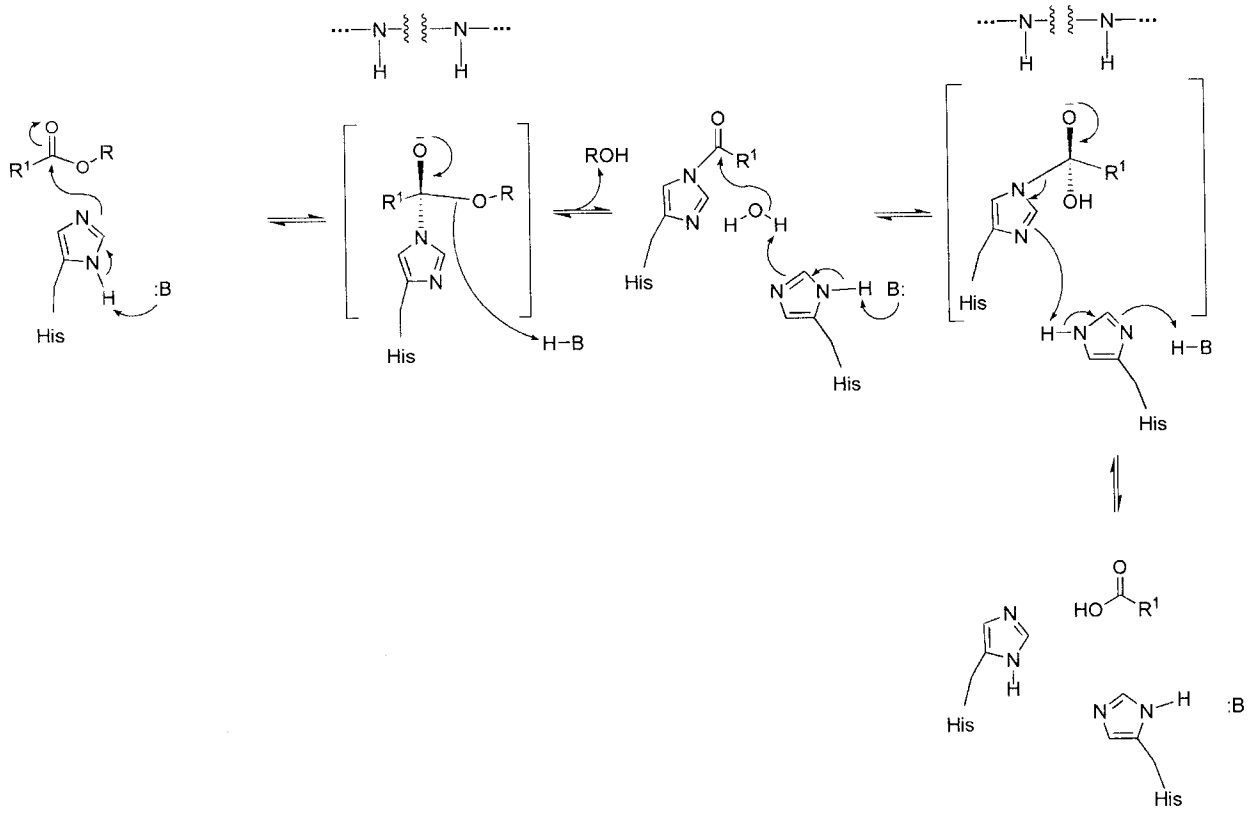

Figure 5-2. Mechanism 2 – Hydrolysis of the ester through formation of acyl-enzyme intermediate

Like Mechanism 1, this is consistent with the residues present in the putative active site of the structural model, mutagenesis studies, as well as being consistent with the low solvent isotope effects observed. However, with the creation of an acyl-enzyme intermediate, one would expect to observe burst kinetics, a phenomenon in which an initial rapid burst phase (corresponding to the formation of the acyl-enzyme complex) would be followed by the slower steady-state rate (corresponding to the hydrolysis of the acyl-enzyme complex). This phenomenon was not observed with EreA or EreB, at least under conditions of the p-NPB continuous assay. Perhaps a burst could be seen under different conditions, or if erythromycin was used as the substrate. However, with the

stopped [^{14}C]erythromycin assay, it was not possible to observe burst kinetics in the time-frame used.

5.2 Future Directions

In order to better evaluate the two possible mechanisms proposed above, some additional experiments need to be done. For example, the capture of an acyl-enzyme intermediate would conclusively determine that the mechanism outlined in Figure 5-2 was indeed occurring. This could be determined by the use of mass spectrometry to detect a species having a mass consistent with the expected acyl-enzyme intermediate, or by detection of radiolabelled enzyme after a reaction of Ere with [^{14}C]erythromycin. If such an acyl-enzyme intermediate was captured, this would show that this mechanism was likely correct, however, failure to obtain such an intermediate would neither prove nor disprove this mechanism, since this intermediate may be very short-lived and difficult to capture.

Additional experiments that could aid in the evaluation of these mechanisms also include further mutagenesis work to see which histidine residues beyond H288 are essential for catalysis. For example, creation of double or triple mutants with combinations of H288A, H46A, and H285A may indicate the involvement of multiple essential histidine residues within the active site.

Since conditions for the crystallization of Ere-bc are known, co-crystallization of the esterase substrate p-NPB with this protein could confirm the location of the active site. Additional structural studies could be pursued with EreA or EreB in order to obtain a 3D structure for an active erythromycin esterase, following up on the initial crystallization screens performed here, as well as pursuing different crystallization

conditions. It is also possible that the other potential erythromycin esterase from *B. cereus*, Bcr135 (PDB 3b55) having the same structure as Ere-bc, may posses erythromycin esterase activity. It would be interesting to further compare the structure of an active erythromycin esterase with both the structure of Ere-bc and our model for EreB.

It was shown here that removal of the tyrosine residue that may block access of erythromycin to the active site of Ere-bc (see Figure 3-4) did not introduce erythromycin esterase activity. It may be, however that Ere-bc could, using the technique of directed evolution, become capable of macrolide inactivation. In this way, random mutagenesis could be used to introduce new substrate specificity. This has been performed for BcII, a metallo-β-lactamase for which DNA shuffling and subsequent rounds of selection resulted in a variant with four mutations yielding the ability to hydrolyze cephalexin, a poor substrate for the wild-type protein (47).

Finally, as genomes from diverse environmental organisms continue to be sequenced, further work may include the investigation of other genes annotated as erythromycin esterases, or whose predicted amino acid sequence similarity to those investigated here may suggest additional proteins that posses erythromycin esterase activity. As erythromycin and other antibiotics continue to be used for clinical therapy against infectious disease, a better understanding of the mechanisms of resistance is critical to our ability to both design new drugs, and effectively use the ones we have.

5.3 References

1. **Anonymous** Comprehensive Microbial Resource - Gene Page BC_3205, Region View. J. Craig Venter Institute [Online.] http://cmr.jcvi.org/tigr-scripts/CMR/shared/GenePage.cgi?locus=NTL01BC3037.

2. **Anonymous** 2007. Streptomyces Database – StrepDB – The Streptomyces Annotation Server SCO_3588. Sanger Institute, UK. [Online.] http://strepdb.streptomyces.org.uk/cgi-bin/dc3.pl?accession=AL645882&serial=3573&width=900&start=3961230&end=3971230&iorm=map

3. **Ackermann, G., and A. C. Rodloff.** 2003. Drugs of the 21st century: telithromycin (HMR 3647)--the first ketolide. J. Antimicrob. Chemother. **51**:497-511.

4. **Andremont, A., G. Gerbaud, and P. Courvalin.** 1986. Plasmid-mediated high-level resistance to erythromycin in Escherichia coli. Antimicrob. Agents Chemother. **29**:515-518.

5. **Arthur, M., A. Andremont, and P. Courvalin.** 1986. Heterogeneity of genes conferring high-level resistance to erythromycin by inactivation in enterobacteria. Ann. Inst. Pasteur Microbiol. **137A**:125-134.

6. **Arthur, M., D. Autissier, and P. Courvalin.** 1986. Analysis of the nucleotide sequence of the ereB gene encoding the erythromycin esterase type II. Nucleic Acids Res. **14**:4987-4999.

7. **Arthur, M., and P. Courvalin.** 1986. Contribution of two different mechanisms to erythromycin resistance in Escherichia coli. Antimicrob. Agents Chemother. **30**:694-700.

8. **Barthelemy, P., D. Autissier, G. Gerbaud, and P. Courvalin.** 1984. Enzymic hydrolysis of erythromycin by a strain of Escherichia coli. A new mechanism of resistance. J. Antibiot. (Tokyo) **37**:1692-1696.

9. **Biskri, L., and D. Mazel.** 2003. Erythromycin esterase gene ere(A) is located in a functional gene cassette in an unusual class 2 integron. Antimicrob. Agents Chemother. **47**:3326-3331.

10. **Blondeau, J. M.** 2002. The evolution and role of macrolides in infectious diseases. Expert Opin. Pharmacother. **3**:1131-1151.

11. **Bolam, D. N., S. Roberts, M. R. Proctor, J. P. Turkenburg, E. J. Dodson, C. Martinez-Fleites, M. Yang, B. G. Davis, G. J. Davies, and H. J. Gilbert.** 2007. The crystal structure of two macrolide glycosyltransferases provides a blueprint for host cell antibiotic immunity. Proc. Natl. Acad. Sci. U. S. A. **104**:5336-5341.

12. **Champney, W. S., and R. Burdine.** 1995. Macrolide antibiotics inhibit 50S ribosomal subunit assembly in Bacillus subtilis and Staphylococcus aureus. Antimicrob. Agents Chemother. **39**:2141-2144.

13. **Cundliffe, E.** 1992. Glycosylation of macrolide antibiotics in extracts of Streptomyces lividans. Antimicrob. Agents Chemother. **36**:348-352.

14. **D'Costa, V. M., K. M. McGrann, D. W. Hughes, and G. D. Wright.** 2006. Sampling the antibiotic resistome. Science **311**:374-377.

15. **Doern, G. V.** 2006. Macrolide and ketolide resistance with Streptococcus pneumoniae. Med. Clin. North Am. **90**:1109-1124.

16. **Douthwaite, S., and W. S. Champney.** 2001. Structures of ketolides and macrolides determine their mode of interaction with the ribosomal target site. J. Antimicrob. Chemother. **48 Suppl T1:**1-8.

17. **Edgar, R. C.** 2004. Mar 19. MUSCLE: multiple sequence alignment with high accuracy and high throughput. Nucleic Acids Res. **32**:1792-1797.

18. **Engel, P. C.** 1977. Enzyme Kinetics: the steady-state approach. Wiley, New York.

19. **Eswar, N., B. Webb, M. A. Marti-Renom, M. S. Madhusudhan, D. Eramian, M. Y. Shen, U. Pieper, and A. Sali.** 2006. Oct. Comparative protein structure modeling using Modeller. Curr. Protoc. Bioinformatics **Chapter 5**:Unit 5.6.

20. **Fett, W. F., H. C. Gerard, R. A. Moreau, S. F. Osman, and L. E. Jones.** 1992. Jul. Screening of Nonfilamentous Bacteria for Production of Cutin-Degrading Enzymes. Appl. Environ. Microbiol. **58**:2123-2130.

21. **Garza-Ramos, G., L. Xiong, P. Zhong, and A. Mankin.** 2001. Binding site of macrolide antibiotics on the ribosome: new resistance mutation identifies a specific interaction of ketolides with rRNA. J. Bacteriol. **183**:6898-6907.

22. **Glucksmann, M. A., T. L. Reuber, and G. C. Walker.** 1993. Nov. Genes needed for the modification, polymerization, export, and processing of succinoglycan by Rhizobium meliloti: a model for succinoglycan biosynthesis. J. Bacteriol. **175**:7045-7055.

23. **Ivanova, N., A. Sorokin, I. Anderson, N. Galleron, B. Candelon, V. Kapatral, A. Bhattacharyya, G. Reznik, N. Mikhailova, A. Lapidus, L. Chu, M. Mazur, E. Goltsman, N. Larsen, M. D'Souza, T. Walunas, Y. Grechkin, G. Pusch, R. Haselkorn, M. Fonstein, S. D. Ehrlich, R. Overbeek, and N. Kyrpides.** 2003. May 1. Genome sequence of Bacillus cereus and comparative analysis with Bacillus anthracis. Nature **423**:87-91.

24. **Kalan, L., S. Ebert, T. Kelly, and G. D. Wright.** 2009. Jul. Noncanonical vancomycin resistance cluster from Desulfitobacterium hafniense Y51. Antimicrob. Agents Chemother. **53**:2841-2845.

25. **Kim, Y. H., C. J. Cha, and C. E. Cerniglia.** 2002. Purification and characterization of an erythromycin esterase from an erythromycin-resistant Pseudomonas sp. FEMS Microbiol. Lett. **210**:239-244.

26. **Leatherbarrow, R. J.** 1992. Grafit 4.2.01. Erithacus Software Ltd.

27. **Levy, S. B., and B. Marshall.** 2004. Dec. Antibacterial resistance worldwide: causes, challenges and responses. Nat. Med. **10**:S122-9.

28. **Lovmar, M., K. Nilsson, V. Vimberg, T. Tenson, M. Nervall, and M. Ehrenberg.** 2006. The molecular mechanism of peptide-mediated erythromycin resistance. J. Biol. Chem. **281**:6742-6750.

29. **Luft, J. R., R. J. Collins, N. A. Fehrman, A. M. Lauricella, C. K. Veatch, and G. T. DeTitta.** 2003. A deliberate approach to screening for initial crystallization conditions of biological macromolecules. J. Struct. Biol. **142**:170-179.

30. **McGuffin, L. J., K. Bryson, and D. T. Jones.** 2000. Apr. The PSIPRED protein structure prediction server. Bioinformatics **16**:404-405.

31. **Mitscher, L. A.** 2008. Coevolution: mankind and microbes. J. Nat. Prod. **71**:497-509.

32. **Nakajima, Y.** 1999. Mechanisms of bacterial resistance to macrolide antibiotics. J. Infect. Chemother. **5**:61-74.

33. **Nakamura, A., K. Nakazawa, I. Miyakozawa, S. Mizukoshi, K. Tsurubuchi, M. Nakagawa, K. O'Hara, and T. Sawai.** 2000. Macrolide esterase-producing Escherichia coli clinically isolated in Japan. J. Antibiot. (Tokyo) **53**:516-524.

34. **Nelson, D. L., and M. M. Cox.** 2000. Lehninger Principles of Biochemistry. W.H. Freeman & Co.

35. **Noguchi, N., A. Emura, H. Matsuyama, K. O'Hara, M. Sasatsu, and M. Kono.** 1995. Nucleotide sequence and characterization of erythromycin resistance determinant that encodes macrolide 2'-phosphotransferase I in Escherichia coli. Antimicrob. Agents Chemother. **39**:2359-2363.

36. **O'Hara, K., and K. Yamamoto.** 1996. Reaction of roxithromycin and clarithromycin with macrolide-inactivating enzymes from highly erythromycin-resistant Escherichia coli. Antimicrob. Agents Chemother. **40**:1036-1038.

37. **Ojo, K. K., M. J. Striplin, C. C. Ulep, N. S. Close, J. Zittle, H. Luis, M. Bernardo, J. Leitao, and M. C. Roberts.** 2006. Staphylococcus efflux msr(A) gene characterized in Streptococcus, Enterococcus, Corynebacterium, and Pseudomonas isolates. Antimicrob. Agents Chemother. **50**:1089-1091.

38. **Oliynyk, M., M. Samborskyy, J. B. Lester, T. Mironenko, N. Scott, S. Dickens, S. F. Haydock, and P. F. Leadlay.** 2007. Complete genome sequence of the erythromycin-producing bacterium Saccharopolyspora erythraea NRRL23338. Nat. Biotechnol. **25**:447-453.

39. **Peano, C., S. Bicciato, G. Corti, F. Ferrari, E. Rizzi, R. J. Bonnal, R. Bordoni, A. Albertini, L. R. Bernardi, S. Donadio, and G. De Bellis.** 2007. Nov 26. Complete gene expression profiling of Saccharopolyspora erythraea using GeneChip DNA microarrays. Microb. Cell. Fact. **6**:37 [Online.] doi:10.1186/1475-2859-6-37.

40. **Plante, I., D. Centron, and P. H. Roy.** 2003. An integron cassette encoding erythromycin esterase, ere(A), from Providencia stuartii. J. Antimicrob. Chemother. **51**:787-790.

41. **Poehlsgaard, J., and S. Douthwaite.** 2002. The macrolide binding site on the bacterial ribosome. Curr. Drug Targets Infect. Disord. **2**:67-78.

42. **Retsema, J., and W. Fu.** 2001. Macrolides: structures and microbial targets. Int. J. Antimicrob. Agents **18 Suppl 1**:S3-10.

43. **Roberts, M. C., J. Sutcliffe, P. Courvalin, L. B. Jensen, J. Rood, and H. Seppala.** 1999. Nomenclature for macrolide and macrolide-lincosamide-streptogramin B resistance determinants. Antimicrob. Agents Chemother. **43**:2823-2830.

44. **Schlunzen, F., J. M. Harms, F. Franceschi, H. A. Hansen, H. Bartels, R. Zarivach, and A. Yonath.** 2003. Structural basis for the antibiotic activity of ketolides and azalides. Structure **11**:329-338.

45. **Schowen, R. L.** 2007. The use of solvent isotope effects in the pursuit of enzyme mechanisms. J Label Compd Radiopharm **50**:1052-1062.

46. **Testa, B., and J. M. Mayer.** 2003. Catalytic mechanisms of hydrolytic enzymes, p. 47-79. Hydrolysis in Drug and Prodrug Metabolism: Chemistry, Biochemistry, and Enzymology. Wiley VHCA, Zurich.

47. **Tomatis, P. E., S. M. Fabiane, F. Simona, P. Carloni, B. J. Sutton, and A. J. Vila.** 2008. Adaptive protein evolution grants organismal fitness by improving catalysis and flexibility. Proc. Natl. Acad. Sci. U. S. A. **105**:20605-20610.

48. **Weisblum, B.** 1998. Macrolide resistance. Drug Resist Updat **1**:29-41.

49. **Wondrack, L., M. Massa, B. V. Yang, and J. Sutcliffe.** 1996. Clinical strain of Staphylococcus aureus inactivates and causes efflux of macrolides. Antimicrob. Agents Chemother. **40**:992-998.

50. **Wright, G. D.** 2005. Bacterial resistance to antibiotics: enzymatic degradation and modification. Adv. Drug Deliv. Rev. **57**:1451-1470.

51. **Wright, G. D.** 2007. The antibiotic resistome: the nexus of chemical and genetic diversity. Nat. Rev. Microbiol. **5**:175-186.

52. **Yong, D., M. A. Toleman, C. G. Giske, H. S. Cho, K. Sundman, K. Lee, and T. R. Walsh.** 2009. Characterization of a new metallo-beta-lactamase gene, bla(NDM-1), and a novel erythromycin esterase gene carried on a unique genetic structure in Klebsiella pneumoniae sequence type 14 from India. Antimicrob. Agents Chemother. **53**:5046-5054.

53. **Zaman, S., M. Fitzpatrick, L. Lindahl, and J. Zengel.** 2007. Novel mutations in ribosomal proteins L4 and L22 that confer erythromycin resistance in Escherichia coli. Mol. Microbiol. **66:**1039-1050.

54. **Zhong, P., Z. Cao, R. Hammond, Y. Chen, J. Beyer, V. D. Shortridge, L. Y. Phan, S. Pratt, J. Capobianco, K. A. Reich, R. K. Flamm, Y. S. Or, and L. Katz.** 1999. Induction of ribosome methylation in MLS-resistant Streptococcus pneumoniae by macrolides and ketolides. Microb. Drug Resist. **5:**183-188.